

Making Sense of the Fractal Urban Form and Function: An Agent-Based Modeling Approach

by

Fatemeh Jahanmiri

A thesis

presented to the University of Waterloo

in fulfillment of the

thesis requirement for the degree of

Master of Arts

in

Planning

Waterloo, Ontario, Canada, 2015

© Fatemeh Jahanmiri 2015

AUTHOR'S DECLARATION

I hereby declare that I am the sole author of this thesis. This is a true copy of the thesis, including any required final revisions, as accepted by my examiners.

I understand that my thesis may be made electronically available to the public.

Abstract

Despite their complexity, cities exhibit very similar fractal properties in various aspects of their form and function, including their social and spatial profiles. These similarities reveal underlying forces behind the formation and evolution of the cities that bind their interrelated profiles. Discovering these underlying forces is critical in order to achieve a comprehensive science of cities. This study proposes a process-based framework that seeks to explain some observed similarities in the social and spatial profiles of the cities. It hypothesizes that fractal patterns in physical urban form originate from a scale-free structure of socio-economic groups and organizations in the cities. An abstract agent-based model is developed to test the hypothesis by simulating the growth of a virtual city from a limited number of agents to a populated landscape with a fractal pattern. Results from the model analysis justify that the aggregate fractal pattern in the urban form can originate from a scale-free distribution of group sizes in the cities, which is in turn a result of preferential attachment in the human aggregation process. The model illustrates that the fractal dimension of the distribution of buildings varies based on the population growth rate, the human interaction rate, and the transportation cost. The findings of this research show that by measuring the fractal dimension of urban forms, we can infer the general pattern of human aggregation structures, including the distribution of activity groups in cities. Acknowledging this relationship may encourage planning and governance to approach attempts to achieve large-scale changes in urban form from the gateway of socio-economic structures and group formation processes. The thesis result motivates further investigation into the relationships between the social group formation process and the compactness and efficiency of cities. Future direction of this work studies the empirical relationships between urban structure and the structure of social networks.

Acknowledgement

I wish to take this opportunity to acknowledge the support of individuals without whom the completion of my thesis would not be possible. First and foremost, I would like to thank my supervisor, Dr. Dawn Parker, who directed my ideas toward a concrete research question and encouraged me to land my thesis through the fluctuations of my Master's journey. Her intellectual guidance and motivation had a great influence on my academic achievements. My special thanks goes to my committee member, Prof. Pierre Filion for reading my thesis, sharing his pearls of wisdom and supporting my research with enthusiasm. Also, I would like to thank the external examiner of my thesis, Dr. Johanna Barros from University of London, U.K., for her valuable time, insights and feedback.

I was delighted to be a member of the Agent-Based Modeling working group, an opportunity provided by Waterloo Institute of Complexity and Innovation (WICI), to meet with peers and interchange ideas. In particular, I am grateful to Dr. Xiongbing Jin, for sharing his technical expertise and helping me in computer modeling and visualization. Also, I would like to thank Nick Guenther and Pedram Fard for assistance with statistical and GIS modeling. My fellow students and friends helped to create a great rewarding experience here at the University of Waterloo. Specifically, I would like to thank Milton Friesen for his valuable feedback and Christina Mora for her astounding editing at short notice.

This research was partially and financially supported by Ontario Graduate Scholarship (OGS), US National Science Foundation CNH-0813799.

Finally, and above all, I like to appreciate my family, specially my beloved husband, Dr. Ali Zibaenejad, for his love, sacrifice and persistence throughout my journey and when the tasks seemed intense and challenging. The completion of my thesis would not be possible without his support. Also, I sincerely thank my mother for her unconditional love and prayers and my father Prof. A. Jahanmiri, for supporting my mission to the last minute of his fruitful life. I praise God for having these people and for all the blessings, which he has given me during my studies.

Table of Contents

| | |
|--|-------------|
| AUTHOR'S DECLARATION | II |
| ABSTRACT | III |
| ACKNOWLEDGMENT | IV |
| TABLE OF CONTENT | V |
| LIST OF FIGURES | VIII |
| LIST OF TABLES | X |
| CHAPTER 1: INTRODUCTION | 1 |
| CHAPTER 2: LITERATURE REVIEW | 8 |
| 2.1 INTRODUCTION TO FRACTALS..... | 8 |
| 2.2 FRACTAL PROPERTIES | 10 |
| 2.2.1 Irregularity | 10 |
| 2.2.2 Self-similarity and scale-invariance | 11 |
| 2.2.3 Power-Law Distribution..... | 12 |
| 2.3 FRACTAL DIMENSION MEASUREMENT..... | 13 |
| 2.3.1 Perimeter-Area Fractal Dimension | 14 |
| 2.3.2 Box-counting Fractal Dimension..... | 14 |
| 2.3.3 Radial Fractal Dimension | 15 |
| 2.3.4 Rank-size Fractal Dimension..... | 16 |
| 2.4 FRACTAL APPLICATION IN URBAN SCIENCE AND PLANNING | 19 |
| 2.4.1 Urban clusters by characteristics | 20 |
| 2.4.2 Fractal Application in Visual Planning and Design..... | 24 |
| 2.4.3 FRACTAL APPLICATION IN URBAN MODELING..... | 25 |

| | |
|---|---------------|
| CHAPTER 3: KITCHENER-WATERLOO CASE STUDY | 31 |
| 3.1 SYNTHETIC LANDSCAPES | 31 |
| 3.2 KITCHENER-WATERLOO CASE STUDY | 36 |
| 3.2.1 Maps and Data | 37 |
| 3.2.2 City-scale scaling analysis | 39 |
| 3.2.3 Intera-urban Scaling Analysis | 41 |
| 3.2.4 Discussion and Conclusion..... | 45 |
| CHAPTER 4: MODEL FRAMEWORK..... | 47 |
| 4.1 GOAL OF MODELING | 47 |
| 4.2 AGENT BASED MODELS | 48 |
| 4.2.1 Netlogo® | 49 |
| 4.3 MODEL DESIGN | 50 |
| 4.3.1 Model assumptions..... | 55 |
| CHAPTER 5: RESULTS | 57 |
| 5.1 INITIAL SETTINGS, AND MODEL SCHEDULE | 57 |
| 5.2 MODEL LANDSCAPE AND RESULT ANALYSIS: | 59 |
| 5.3 MODEL VERIFICATION..... | 62 |
| 5.3.1 Null Hypothesis | 64 |
| 5.4 EXPERIMENTS | 67 |
| 5.4.1 Effect of Population Growth Rate on the Model Landscape | 67 |
| 5.4.2 Effect of Vision-Radius on the Model Landscape | 69 |
| 5.5 DISCUSSION | 72 |
| CHAPTER 6: CONCLUSION | 75 |
| 6.1 Study Overview..... | 75 |
| 6.2 Future Direction | 76 |

| | |
|--|----|
| 6.3 Planning and Policy Implications | 77 |
| BIBLIOGRAPHY..... | 79 |
| APPENDIX 1: FRACTAL METRICS..... | 84 |
| APPENDIX 2: SIZE-DISTRIBUTION OF URBAN FORM IN KITCHENER-WATERLOO..... | 86 |

List of Figures

| | |
|--|----|
| Figure (1-1): Conceptual diagram of the thesis hypothesis development | 5 |
| Figure (2-1): Illustration of the coastline paradox..... | 8 |
| Figure (2-2): The dimensional continuum of fractal form..... | 9 |
| Figure (2-3): Self-similarity in fractals | 11 |
| Figure (2-4): An example of power-law distribution in a simple fractal structure | 12 |
| Figure (2-5): Box-counting fractal dimension of the coastline of Britain | 15 |
| Figure (2-6): Example of a fractal tree formation and calculation | 18 |
| Figure (2-7): Literature map on fractal applications in urban planning..... | 19 |
| Figure (2-8): Illustration of figures with the same density but different fractal dimension..... | 20 |
| Figure (2-9): The correlation between fractal dimension and urban form texture | 22 |
| Figure (2-10): Initial analysis of building heights in New York, Tokyo, and London | 26 |
| Figure (2-11): Time series representing land use distribution of a simulation results | 29 |
| Figure (3-1): Synthetic landscapes' pattern-generator elements..... | 32 |
| Figure (3-2): Synthetic landscapes demonstrating various initial conditions | 32 |
| Figure (3-3): Graphs representing power distribution of element sizes in synthetic landscapes..... | 34 |
| Figure (3-4): Kitchener-Waterloo urban wards | 37 |
| Figure (3-5): Log-Log graph of road length frequency in Kitchener and Waterloo..... | 40 |
| Figure (3-6): Log-Log graph of parcels length frequency in Kitchener and Waterloo | 40 |
| Figure (3-7): Log-Log graph of buildings length frequency in Kitchener and Waterloo..... | 40 |
| Figure (3-8): Neighborhoods with power-law distribution for parcels and roads | 43 |
| Figure (3-9): Neighborhoods with power-law distributed buildings..... | 44 |
| Figure (3-10): Bridgeport Neighborhood in Kitchener with roads and building footprints..... | 45 |
| Figure (4-1): Model's key elements: growth, aggregation, and allocation processes..... | 48 |

| | |
|--|----|
| Figure (4-8): Main pseudo code block of the model | 55 |
| Figure (4-3): Main pseudo code block of the model | 54 |
| Figure (5-1): Model interface in Netlogo® | 58 |
| Figure (5-2): Model outcome landscape in Netlogo®..... | 59 |
| Figure (5-3): Voronoi Illustration of Parcel Distribution in Simulated City..... | 60 |
| Figure (5-4): Rank-Size distribution of buildings by area | 61 |
| Figure (5-5): Distribution of R-squared for the power law tests | 63 |
| Figure (5-6): Distribution of fractal dimension of verification tests | 64 |
| Figure (5-7): Simulated landscape from null hypothesis revealing dispersed size distribution | 65 |
| Figure (5-8): Radial Distribution of buildings in the null hypothesis..... | 66 |
| Figure (5-9): Rank-Size distribution of buildings sizes for the null scenario | 66 |
| Figure (5-10): Rank-size distribution from the tests of different Population Growth Rates | 67 |
| Figure (5-11): Rank-size distribution of buildings in the experiment landscapes | 69 |
| Figure (5-12): Diagram showing the experiment vision value in reference to CBD | 71 |

List of Tables

| | |
|---|----|
| Table (1-1): Power Law phenomena in social and spatial profiles of cities in the literature | 2 |
| Table (3-1): power law properties of four synthetic landscapes | 34 |
| Table (3-2): Neighborhood names and codes in KW | 38 |
| Table (3-3): Fractal dimensions for roads, parcels and buildings in KW | 39 |
| Table (3-4): Fractal dimension of parcels' size distribution in Kitchene..... | 42 |
| Table (3-5): Fractal dimension of roads' length distributions in Kitchener-Waterloo..... | 43 |
| Table (3-6): Fractal dimension of buildings' size distributions in Kitchener-Waterloo..... | 44 |
| Table (5-1): Model parameter range and 'base case' values | 58 |
| Table (5-2): Power law parameters of regression analysis for buildings distribution | 61 |
| Table (5-3): Experiment results for variation of population growth rate | 68 |
| Table (5-4): Fractal dimension of simulated landscapes for vision experiments | 70 |

Chapter 1: Introduction

For centuries, urban scholars have been wondering what constitutes good urban form (Lynch, 1960). Thousands of theories and ideologies have been developed and practiced based on the perception of a *Perfect City*. Such theories vary from The Garden City to Technological Utopias to The New Urbanism (Pinder 2013), most of which focus on the physical *form* and *design* as their targets. However, achieving functional goals has always been the main challenge of most of these design-oriented theories. Thus, concern was shifted to understanding the extent to which urban planning and design are able to influence urban form and function (Fainstein 2000).

It wasn't until the late twentieth century that the traditional notion that explains the city as a machine that performs in the way we design it was replaced by the complex systems approach (Manson 2001; Batty & Marshall 2011). The complexity of cities implies that their form emerges from the bottom up as the result of interconnected variables (Batty, 1994). We now know that urban form is fractal, suggesting that the irregular patterns in the built environment repeat in every scale, and has a power law distribution of component sizes. Despite several studies that suggest theoretical methods that generate fractal forms (Batty 1991, White & Engelen 1993), the underlying process responsible for fractal patterns in evolution of urban form remains a mystery.

Recently, the ability to obtain and analyze large-scale data on several aspects of cities has provided us with new insights into the spatial complexity of urban dynamics. Evidence from many empirical studies suggests that there is a common power law relation in the urban statistical properties, including both infrastructural size distribution such as roads and buildings (Batty 2008), as well as socioeconomic activities such as firms and organizations (Andriani & McKelvey 2009; Farmer & Geanakoplos 2008). Some of the more relevant studies from both built environment and socio-economic profiles of cities are listed in Table (1-1). The presence of a power law behavior in

the size distribution of elements of a system implies self-similarity in its underlying system dynamics (Batty & Longley, 1994). Furthermore, a power law distribution is one of the dominant characteristics of fractal objects, and in general complex systems.

Although linkages between fractal urban form and city function have been explored (Frankhauser 2008; Bettencourt 2013), the causal associations between power-law socioeconomic structures and fractal urban form have not. For example, there have been attempts to derive the origin of this interdependence in urban properties by proposing mathematical frameworks that links global patterns to few basic local parameters such as population (Bettencourt, 2013). However, the explicit underlying chain of processes that causes similar statistical properties in socioeconomic and spatial urban aspects has remained unknown.

Table (1-1): Power Law phenomena in social and spatial profiles of cities in the literature

| Phenomena | Source |
|----------------------------------|--|
| Socio-Economic Profiles | |
| Hierarchy of social group size | (Zhou, Sornette, Hill, & Dunbar, 2005) |
| Job vacancies | (Gunz, Bergmann Lichten, & Long, 2002) |
| Social networks | (Watts, 2004) |
| Firm size (by revenue) | (Axtell, 2001) |
| Firm Size by number of employees | (Aoyama, Yoshikawa, Iyetomi, & Fujiwara, 2009) |
| Built Environment | |
| Parcel size by area | (Fialkowsky and Bitner 2008) |
| Building footprint area | (Batty, 2008; Samaniego & Moses, 2008) |
| Length of road network | (Samaniego & Moses, 2008) |

Identifying the origin of the linkages between different facets of the city is essential to understand urban dynamics, which contribute to the evolution of urban form. Such identification would also helps to design effective interventions. In search of this origin and by mapping the observations of the above studies, I propose a unified hypothesis that helps to explain why these similar patterns emerge. I use three simple assumptions to construct the hypothesis:

1) People are the essence of change; cities change because the people living in them change.

In other words, the form of a city does not change unless human beings, their needs, and their actions make changes in the social and physical aspect of cities. As such, the city can be considered to have a sole living entity, which is the people connected together; each of its social, economic, and physical profiles can be interpreted as only one layer of this entity.

2) External and internal forces: There are two sets of forces that define the next state of any change in the urban environment: first, internal forces, which initiate from people, their needs, preferences and actions, and second, external forces, which are applied from the built or natural environment. The reactions of human being to the potentials, threats, and constraints of the environment define the way the city evolves through time. Any other factor can be classified in one of these two groups. For example, weather conditions, proximity to geographical features, topography, and other environmental factors are all considered as external forces. Thus, the city is a reflection of its people through the lens of its environment, and these two are inseparable.

3) Buildings are the containers of human activities. Each building in a city can be seen as a home to the activities of an individual or a group of people. It can either be a house for a family, a retail store for a group of people to shop, an office building for an organization, or a shopping mall that serves an urban district. The characteristics of buildings (such as function and location) reflect the characteristics of their users to a great extent. One of the main determinants of this reflection is the size match. Generally, depending on how large the number of users is, the floor area of the building varies. However, the degree of this reflection varies among geographical locations and cultures.

Consideration of the relationship between building characteristics, or in more general terms, the characteristics of the urban physical environment and human activities, is essential to understand urban dynamics. For clarification, I dig into more detail about the process that leads to transformation of the built environment: the construction of a new building. Imagine a typical

building in a typical city. Before the building is built, it had enough demand to be created and designed. Its design process takes place under users' demands and budget. The users are a social unit that can be an individual, a family, a group, a firm, an organization or any kind of association that needs a space for their activities and have enough power (or resources) to own a building. For simplicity, I will assume that all of these possible social units that can occupy a building are each a kind of group; either a group of one, or a group of more than a thousand people, but I will call them "groups" for now. Although the formation process of these groups varies significantly from case to case, in general, there are two main logics involved: first, physically closer individuals or groups are more likely to join together compared to distant ones. Second, larger groups are more likely to attract new members compared to smaller ones. Based on these two basic aggregation principles, individuals unite gradually and form associations that will later settle in buildings.

As the buildings are the containers of groups, larger groups require larger buildings. That is the size of the required building for a group is an increasing function of the size of that group (size, here, refers to the number of members or individuals that are associated with a particular group). For example, a company with 500 employees needs a larger parcel and a larger building for its functionalities compared to a company with 50 employees. It is important to note that the reverse side of this statement is not always true; that is, larger buildings are not necessarily owned by larger groups. In this study, we focus on the former process per se (groups with larger number of members need larger buildings to settle in). Furthermore, this assumption takes into account the fact that neither every social unit needs a building for its functions nor it attains the power to possess one¹.

¹ For example, while a group of neighbors may form a community and need a community center for their activities, they might not succeed in achieving one. Also, a group of friends who are connected by social media does not even need a physical space unless they have a mission significant enough for investment, which leads to creating a firm or an institution accordingly. Hence, a group has to be sustained and stable enough to become a candidate for making a physical change in the built environment.

Thus in the model, only groups that need a space for their activities (such as employment groups) are modeled.

In fact, numerous factors are involved in determining the relation between size of a building and size of the group that is using it. These factors include but are not limited to: activity type, frequency of use, zoning, density and land price. However, the existence of these factors and their role in defining the size of each building as a function of its users does not modify the dominant effect of number of members in each group, which is the first and foremost determinant of building capacity.

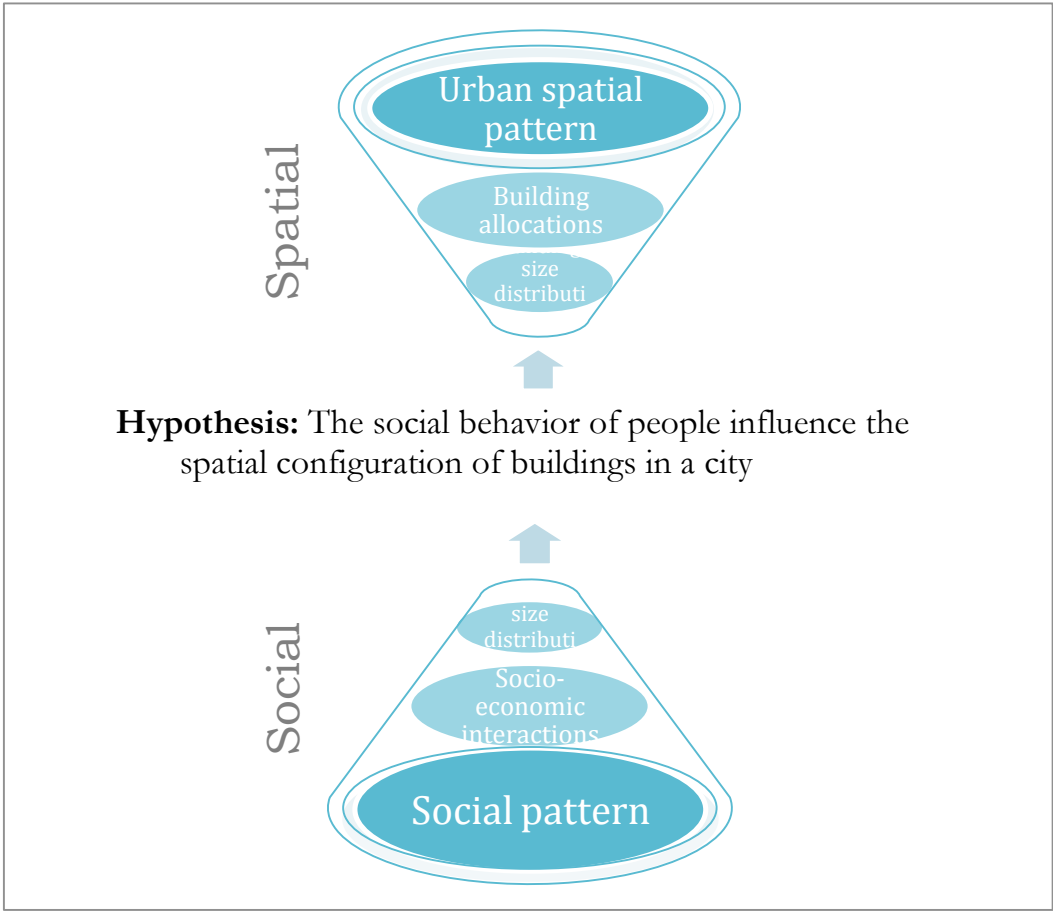


Figure (1-1): Conceptual diagram of the thesis hypothesis development. Narrowing down the social and spatial structures of cities into size distribution of buildings and groups, the linkage is derived theoretically.

Based on the above preface, I propose a integrative deductive theory of how social and spatial interdependencies arise. The theory connects the social and spatial structure of cities by

refining each side into some measurable phenomena. As illustrated in the above diagram, the hypothesis is based on the similarities of size distribution of groups and buildings, each as a representative of a more general concept. It hypothesizes that group size distribution represents the structure of socio-economic interactions, which in turn represents the social pattern of the city in general. Also, the buildings size distribution represents the spatial pattern of the built environment. The way I narrow down the two general social and spatial patterns and use the hypothesis to connect them is shown in Figure (1-1). The theory states that the same overall distribution pattern as in the social group sizes is also reflected in the distribution of building sizes in a city. It asserts that the observed power-law patterns in the distribution of building sizes are rooted in the distribution of associations of people who use the buildings. It also applies to the spatial configurations of building in the city, where larger buildings are more concentrated in areas where larger groups of people interact.

The approach of this study is to model the chain of processes that lead to formation of the built environment and to show how scale-free patterns emerge in social systems and pass to physical systems. For this purpose, an agent-based model of an archetypical city is developed in Netlogo[®], which simulates the growth of a city from a single seed in space to a large urban landscape with fractal properties. The processes that are modeled can be summarized in three phases: human interaction, group formation, and building allocation. More details on these phases and the structure of the model are provided in the proceeding section.

Further, I test the model using various parameter settings to explore the effect of aggregation and segregation forces and present the outcome in the result section. All model results support the hypothesis strongly by revealing patterns that are similar to real-world urban patterns. Regression analysis on the distribution of buildings in the outcome landscapes shows clear power-

law relations with different slopes due to varying parameters. The radial distribution analysis of building sizes reveals characteristics similar to real-world radial distribution pattern.

The results of this study highlight the central role that human interactions play in defining the way cities form and spread on landscape. They further help planners to distinguish the underlying driving forces of urban form by examining the patterns in the size distribution of buildings in a city. The proposed theory is also consistent with the principles of advocates of planning for people, who believe that any planning intervention should be small scale, gradual and based on public participation in order to be successful (Jacobs, 1961; Mumford, 1937; Robinson et al., 2007).

The thesis is organized into the following chapters: Chapter 2 provides a general definition of fractal theory and fractal measurement methods followed by an overview of the literature that applies fractal measurements in urban studies. Chapter 3 is dedicated to a case study, where I used fractal dimension to measure the complexity of built-up areas in Kitchener-Waterloo cities. In Chapter 4, I construct an agent-based model to test the hypothesis discussed in the current chapter. The model is then implemented and the results are presented in Chapter 5 along with related discussions. Conclusion and future direction is discussed in Chapter 6.

Chapter 2:

Literature Review

2.1 Introduction to fractals

The term fractal was first coined by Mandelbrot in 1975 to describe geometry of natural forms such as branches of trees, surfaces of mountains, and the shape of coastlines. Mandelbrot defines fractals as “mathematical objects, whether naturally or man-made, which can be described as irregular, coarse, porous or fragmented, and which furthermore possesses these properties to the same extent on all scales” (Mandelbrot 1975). Fractals are made up of parts that resemble the whole in some way, so if one zooms in on a fractal object, the same form reoccurs over and over.

Fractal objects cannot be defined or measured using the Euclidean geometry. Mandelbrot referred to the example of the coastline paradox to elaborate on the property of fractal forms and the deficiency of classic geometry to define them. He shows that the length of the coastline of Britain depends on the scale of measurement, and thus coastlines do not have a well-defined length,



Figure (2-1): Illustration of the coastline paradox. From left to right, the coastline of Britain is measured by 200 km, 100 km, and 50 km rods, resulting in 2350 km, 2775 km and 3425 km length of coastline respectively (Van de Sande, 2004).

as demonstrated in Figure (2-1). However, if the coastline is examined as fractal, the measurement paradox is resolved because the coastline curves repeat themselves in every scale and thus, the length

can vary depending on the measurement scale dimension. Measuring the coastline using a fractal provides a constant number, which defines the shape of the coastline based on the amount of details it has in every scale and the way it has filled the space available to it (Mandelbrot, 1990).

The main distinction between fractal and Euclidean geometry is the dimension in which the form is constructed. For example, lines, circles, and cubes, have integer dimensions of one, two and three respectively. They can also be described, aside from their position, by only one or two parameters, such as length or radius, which are a scale of length. However, fractal forms have dimension that is a *fraction* of the integer numbers and falls between classical dimensions as illustrated in Figure (2-2) below (Batty & Longley, 1994). For this reason, their dimension is called

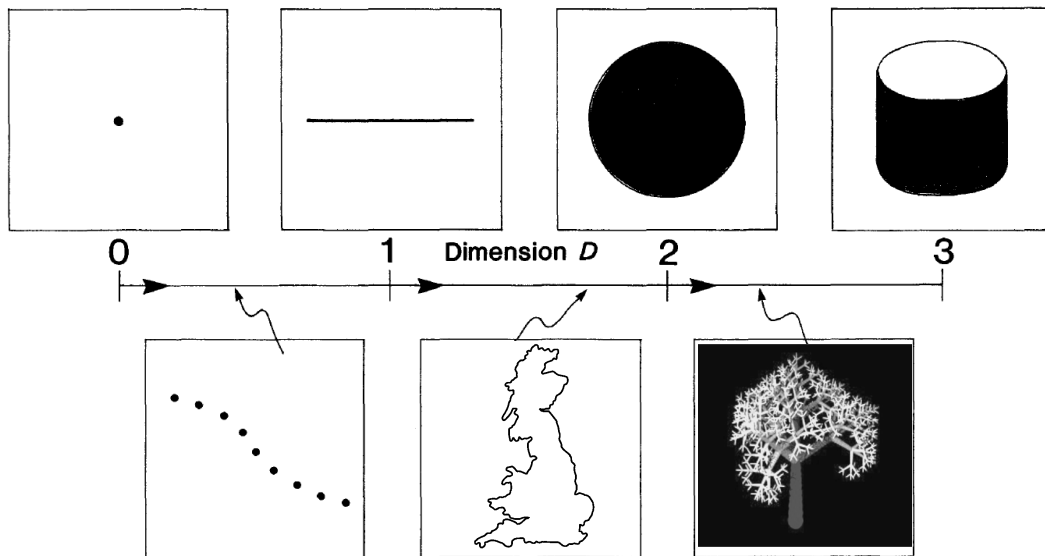


Figure (2-2): The dimensional continuum of fractal form in regard to dimensions of point, line, plane, and three dimensional forms in Euclidean geometry. (Retrieved and modified from (Batty & Longley, 1994))

fractal dimension. Fractal dimension is defined as the ratio between object properties of any consecutive scales of measurement, which is constant across varying scales. In fractal geometry, the fractal dimension can also be interpreted as the extent to which the form has filled the space available to it. In the above examples provided in Figure (2-2), the coastline of Britain has a fractal dimension between one and two, which exceeds the dimension of line but has not filled the space as

much as a plane. Similarly, the computer-generated model of a tree, as in Figure (2-2), has a fractal dimension between two and three and will be close to three the more densely the branches are spaced. Fractal dimension is defined and measured differently based on the property that is being measured (Mandelbrot, 1990). More discussion on definition of fractal dimension and ways of measuring it is provided later in Section 2.3.

2.2 Fractal Properties

Fractal objects can be classified in two general categories: mathematical fractals that are generated by humans, and natural fractal forms that are observed in real world. The properties of fractals are slightly different in each category. I discuss the key fractal properties in the following sections.

2.2.1 Irregularity

The first and foremost property of fractals is irregularity, known as the opposite of smoothness, which refers to properties of broken uneven shapes that cannot be described by Euclidean geometry. Both natural and mathematical fractals exhibit irregular patterns at every scale of observation. Consequently, fractal dimension has paved the way for scientists to define and measure geographic features, urban boundaries, and urban footprints, despite the irregularity of their form. In the example of the coastline of Britain provided earlier, the irregularity of the coastline is the cause of measurement paradox. More specifically, each segment of the coastline needs to be simplified to fit the classic geometric models, such as a line, to be measurable, and thus is highly dependent on the scale of measurement. Although irregularity is one of the most ill-defined properties in mathematics, there have been some methods developed to define the irregularity of fractal shapes, such as perimeter-area dimension. In Section 2.2.1, the Perimeter-Area dimension, as an example of these methods is introduced.

2.2.2 Self-similarity and scale-invariance

Fractal objects are self-similar in the way their shape resembles their parts in arbitrary scales. Self-similarity may be manifested as being exact, approximate, statistical, or qualitative. Exact self-similarity, as its name suggests, refers to an object that has identical shapes in any scale. Deterministic mathematical fractal structures, such as the well-known Koch snowflake curve illustrated in Figure (2-3)-(a), exhibit exact self-similarity in every scale. However, in approximate self-similar objects, local patterns resemble global patterns, but are distorted in some ways. This property is evident in stochastic mathematical fractals such as Mandelbrot set, and most natural fractal structures such as trees or the shape of the coastline of Britain (Falconer, 2013).

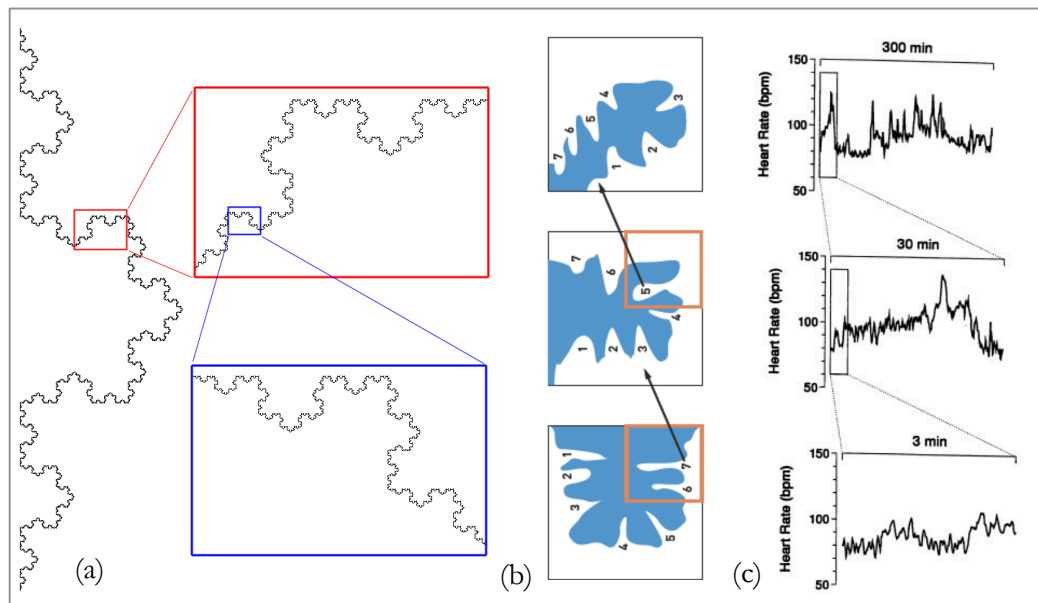


Figure (2-3): Self-similarity in fractals. (a): exact self-similarity in the Koch Curve fractal. (b): approximate statistical self-similarity in fractal pattern of a coastline. The diagram shows a simplified example of coastline shape in three scales and show that although, the exact shape is not repeated in different scales, the overall pattern such as the number of bays and valleys are approximately resembled. (c): Qualitative self-similarity in fractal temporal process of heart rate regulation. (The illustrations are respectively adopted from Bourke (2003); Annenberg Foundation (2014); Goldberg et al. (2002).)

Self-similarity of fractal systems not only describes the spatial structures, but also, can be used to define the statistical and qualitative attributes of such systems. For example, statistically self-similar objects have the same statistical properties such as frequency of components, fluctuation

pattern, and number of peaks and valleys across all scales (e.g. Figure (2-3)-(b)) (Falconer, 2013). The size distribution of buildings, parcels and roads in a city are also an example of statistical self-similarity, as will be discussed further later in this chapter. Last, but not least, qualitative self-similarity is referred to as a non-spatial or non-geometric series that has repeated attributes, such as time series (Falconer, 2007). The fluctuation pattern of human heart rate, for example, is illustrated in Figure (2-3)-(c) and shows that the heart-rate variation in 300-minute period resembles the 30-minute and 3-minute periods (Goldberg, et al., 2002).

2.2.3 Power-Law Distribution

The distribution of elements or segments in a fractal set follows a power law relation, implying that the frequency of components of certain size scales by a constant factor as shown below:

$$N(\epsilon) = a/\epsilon^\alpha \tag{2-1}$$

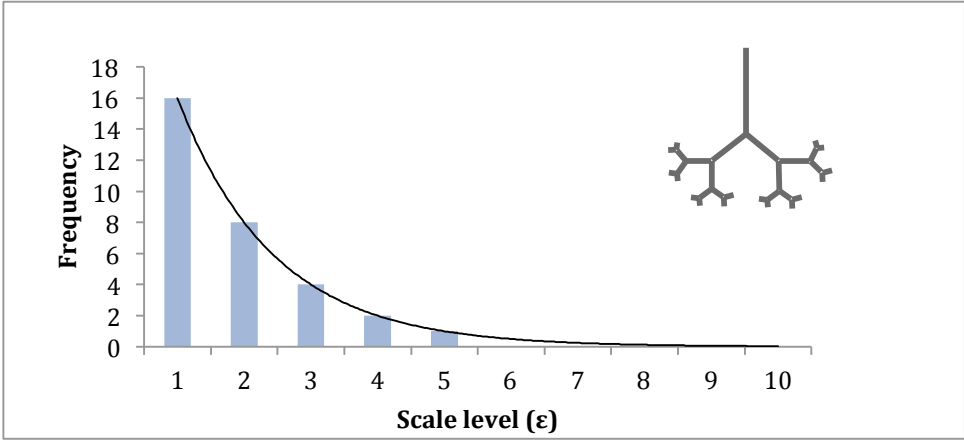


Figure (2-4): An example of the power-law distribution of component sizes of a simple fractal structure.

Here, N refers to the number of components of size ϵ in the system, and α represents the scaling exponent. Figure (2-4), provides an example of the distribution of element sizes of the given tree-like fractal structure. The X axis represents the scale size variable, usually provided in bins for empirical data, which have not perfectly-sized components. The Y axis represents frequency of

components of that size. Informally, a fractal set has many small size components, some mid-range values and only a few extremely large values. In a more general sense, a power law distribution states that variable Y will decrease hyperbolically with an increased value of X (Cioffi-Revilla, 2003). Thus, a power-law relation is generally presented in a log-log graph to show the distribution fit into a linear model. The slope of the line defines the scaling factor, which is directly used to derive fractal dimension. It is important to note that all fractals follow a power law probability distribution, but the reverse side of this statement is not always true. That is, not all systems with power-law distributed probability are considered as fractal, because their spatial configuration may not necessarily have a hierarchical relationship. In general, power law or scale-free distribution is referred to a constant proportional relationship between entities of different sizes. If such scaling property holds through topological or spatial relationships in a system, then it is called fractal. The fractal dimension is derived from the scaling factor (α), depending on the fractal type and the context that it is studied. Hence, a power-law regression analysis provides preliminary evidence of fractal properties of an entity, but does not guarantee it (Dauphiné, 2013). The methods of calculating fractal dimension based on the power-law are discussed in the next section.

2.3 Fractal Dimension Measurement

The definition of fractal dimension varies significantly in different disciplines depending on the type of fractal under study. Consequently, there is no agreement among physicists, mathematicians and geographers on a unified method of calculating fractal dimension. In this section, I focus on three categories of fractal dimension calculating methods that are common in analyzing urban phenomena (Dauphiné, 2013). The classification of these methods is based on the type of data that is explored including: black and white maps, landscape images, and frequency series of size, value and time. These methods include: box-counting, radial fractal dimension and rank-size fractal dimension.

2.2.1 Perimeter-Area Fractal Dimension

One of the very first measurements to describe the irregularity of fractal objects is perimeter-area fractal dimension (PAF). As such, PAF is calculated as the ratio of the logarithm of perimeter to the logarithm of area as in equation (2-2) below:

$$P = CA^{\frac{D_p}{2}} \quad \text{or,} \quad D_p = 2C \cdot \frac{\log P}{\log A} \quad (2-2)$$

Here, D_p denotes the perimeter-area fractal dimension, P refers to perimeter, A states the area and C is the shape constant (embedded into two-dimension). So, the higher, the ratio of perimeter to area, the more irregular the shape is (Mandelbrot, 1984). Notably, PAF can only be used upon physical objects that have defined perimeter and area and so can't be used to describe a fractal system composed of several components.

2.3.2 Box-counting Fractal Dimension

Box-counting is the most classic approach to calculate fractal dimension of black-and white maps that distinguish buildings from open space in binary form. The basic mechanism used in this method is that a mesh of boxes of size ε is traced over the map or image under study. Then, the number of boxes that intersect with the black pixels is measured. This process is repeated for increasing values of ε , and the numbers of pixels for each tracing are recorded. The data is then represented on a graph with the box size measurements on the X-axis, and number of cells counted on the Y-axis. In a fractal form, such graph reveals a power-law relation with slope of

$$\alpha = D_E - D_F \quad (2-3)$$

where, D_E is the Euclidean dimension of the shape (which equals to 2, in maps and images), and D_F denotes the box-counting fractal dimension (Batty & Longley, 1994; Thomas I., 2010).

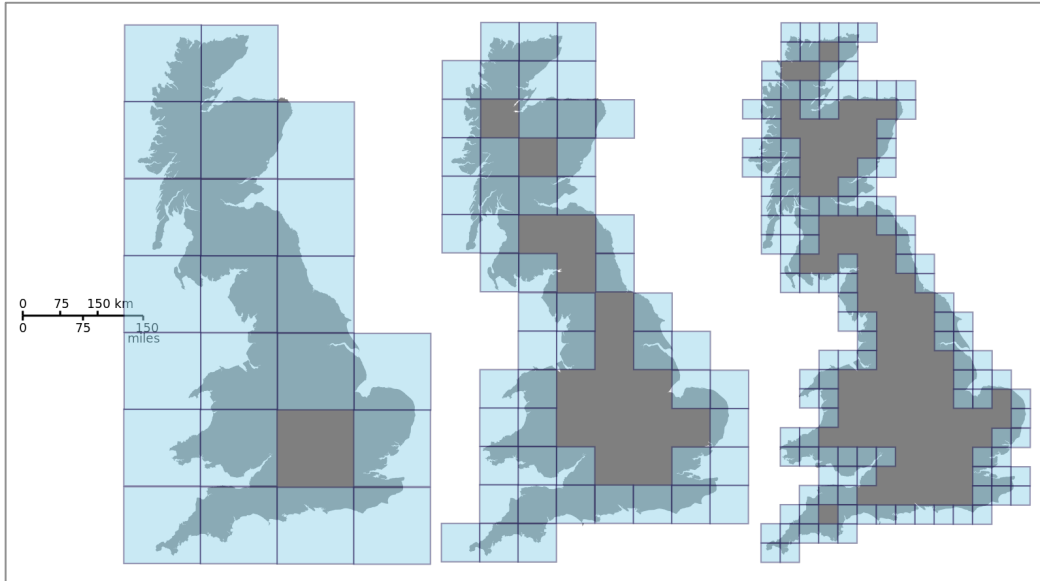


Figure (2-5): Box-counting fractal dimension of the coastline of Britain. (Adopted from (Prokofiev, 2013))

The box-counting method can also be employed to measure the fractal dimension of landscape images. The image is first saved as a gray-scale image, and then, the difference between minimum and maximum gray-scale values is calculated for each box. Then, the data are plotted in a graph with box sizes in the X-axis and the differences between gray-scales values in each box in the Y-axis. In a fractal landscape, the structure of this graph can be estimated with a power law model. The fractal dimension derived from this technique is always a measure of the irregularity of the object, but the self-similarity needs to be verified in advance (Dauphiné, 2013).

2.3.3 Radial Fractal Dimension

Radial fractal dimension is another fractal measurement that deals with maps and images. The main application of radial fractal dimension is to examine the fractal pattern in distribution of a population around a central point. It has been shown that in a self-similar city with a central growth core, the urban density at distance r from the center is:

$$\rho(r) = \rho_1 r^{D_f - d} = \rho_1 r^{-a} \quad (2-4)$$

where ρ_1 is the proportionality coefficient, a refers to the scaling exponent of density distribution, d is the Euclidean dimension (which equals to 2 in two-dimensional maps and images), and D_f denotes the radial fractal dimension of urban form, which should be smaller than the Euclidean dimension (Batty & Longley, 1994). Due to the extensive transformation of many cities from monocentric to polycentric structures, there have been studies that developed the radial dimension methods to encounter fractal patterns of polycentric cities (Chen, 2013a); however, covering these methods is beyond the scope of the present study.

2.3.4 Rank-size Fractal Dimension

In non-spatial phenomena, that there is no maps or images involved, frequential distributions are used to derive fractal dimension. As discussed earlier, the self-similarity or scale-invariance property in frequential distributions is known as a power-law. Zipf's laws and Pareto distributions, which are examples of power laws, are frequently used for calculating fractal dimension (Newman, 2005). The process of preparing data to estimate Zipf's or Pareto distribution models involves arranging the data in an increasing or decreasing order, which leads to construction of a rank-size graph. Depending on whether the X axis represents ranks and the Y axis represents the size or vice versa, this graph is regarded as Pareto or Zipf's law. These two graphs are equivalent representations of power laws. Zipf's law in particular is employed to analyse the fractal dimension of discrete values. Zipf's law first became popular for analysing the distribution of cities by their population in the US cities. Both X and Y axes of power law graphs are expressed in logarithmic scales, which highlight the linearity of distribution patterns. Thus, to determine the slope coefficient the Zipf's model and Pareto models are stated below in equation (2-5) and (2-6) respectively:

$$\log Rank = \log A - \beta \log Size \quad (2-5)$$

$$\log \text{Size} = \log A - \alpha \log \text{SizeRank} \quad (2-6)$$

The slope coefficient for Zipf's law is β , which is equal to $1/\alpha$. Zipf's law requires that this coefficient needs to be close to 1. The advantage of rank-size distributions over the simple frequency curve is that the shape of the graph is not dependent on the choice of class intervals. The scaling coefficient derived from these equations can be used for fractal dimension with confidence (Dauphiné, 2013).

It is important to exercise caution when analyzing empirical distribution data for power-laws. The reason is that unlike ideal mathematical fractals, natural fractals do not follow a power-law perfectly. This deficit is specifically observed in the head and tail of the distribution graph. Most empirical power-laws have bended heads and fat tails. These are hypothesized to be the result of growth limits and constraints in the fractal process underneath. For example, in case of the city size distribution, settlements smaller than a certain size are not possible or efficient. Also, limited resources as well as environmental constraints slow down the growth of cities to their maximum theoretically expected size. Thus, only the linear part of the rank-size distribution should be estimated as a power-law curve (Dauphiné, 2013).

For clarification, I calculate the fractal dimension of the branching example provided in Figure (2-4). The structure is presented in more detail in Figure (2-6) below including the simplified process that lead to formation of such fractal form. In each iteration the form grows based on two main functions: first, multiplications of the initial form by n , and second, scaling of the initial element size by ε . In fractal forms, n and ε remain the same throughout the whole growth process and develop self-similar structure.

Fractal dimension can be derived from n and ϵ , assuming that the proportion of the two parameters remains constant in every scale of measurement. Thus the fractal dimension, D_f , is calculated as the Equation (2-7) below:

$$D_f - D_E = \lim_{t \rightarrow \infty} \log N(\epsilon) / \log \epsilon \quad (2-7)$$

where D_f refers to fractal dimension and D_E denotes the Euclidean dimension (which equals to 2 as the form is spreading on a plane).

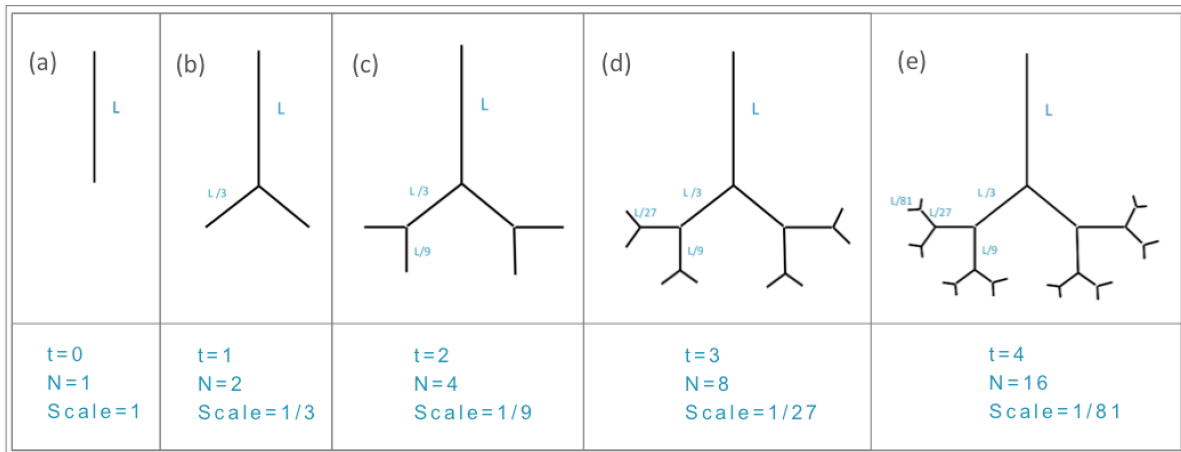


Figure (2-6): Example of a simplified formation process of a fractal tree. t refers to iteration stage, so the form develops as t increases; N refers to the number of branching in the multiplication process, so in each development stage N times the initial number of elements is added; *Scale* refers to the ratio of the new element size to the size of the initial element). So, in the fractal tree above, $D_E - D_f = \lim_{t \rightarrow \infty} \log N(\epsilon) / \log \epsilon = \log 2 / \log 3 = \log 4 / \log 9 = \log 8 / \log 27 = \log 16 / \log 81 = 0.63$. $D_f = 2 - 0.63 = 1.36$

Obviously, this approach is only useful when working with an artificial fractal such as the fractal tree example above, where all the elements added in each iteration have exactly the same size. In natural fractals however, elements of approximately similar size are categorized in a class of size $\epsilon \pm \Delta$ and then, the proportion of all consecutive class sizes are measured. If power law analysis shows that the proportion is constant through every scale of measurement, then Equation (2-7) can be used to define the fractal dimension of the system.

2.4 Fractal Application in Urban Science and Planning

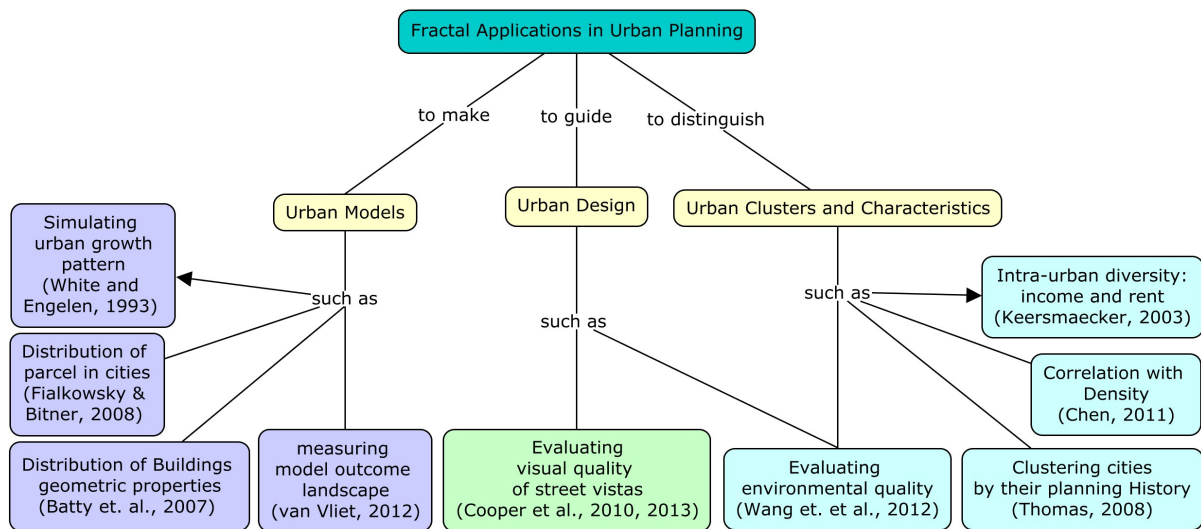


Figure (2-7): Literature map on fractal applications in urban planning. This diagram shows an example of each type of application that is covered in this chapter and does not represent all relevant literature.

Fractal analysis is used as a prevailing tool for quantifying and measuring urban forms. The reason is that city form is mainly characterized by irregularity (as in urban boundaries), self-similarity (as in urban growth patterns), and scaling behavior (as in buildings size distributions (Batty & Longley, 1994)). In this section, a brief overview of the various applications of fractal theory in urban planning and the science of cities is provided. Figure (2-7) indicates a simple map of the literatures that are reviewed here based on their application field to help the reader to see the links between the applications.

In general, studies that have employed fractal dimension as a tool to study urban phenomena can be classified into three categories: clustering similar urban areas based on their characteristics, evaluating and guiding urban design, and modeling cities. Among all different examples of subcategories that can be defined for each application field, key examples are selected for review in the following sections.

2.4.1 Urban clusters by characteristics

Advancements in methods and tools to measure fractal dimension of geographic features and maps have enabled researchers in urban studies to explore the properties of urban forms from new angles (Gil et al., 2012, Chen, 2012; Chen, 2013a,b). The first class of research on the fractal properties of cities has focused on black and white maps of cities, where black represents developed areas, and white indicates the free and natural surrounding lands. Using the box-counting method, the frequency of developed land is measured at different scales and plotted on a logarithmic graph. If the log-log graph reveals a linear structure, and the slope of the best-fitted line falls between 1 and 2, then the city is considered to have a fractal pattern (Batty and Longley, 1994).

Urban Built-up Density

This approach has been used as an instrument to describe the physical characteristics of cities. For example, in a study of the periphery of Brussels, Thomas et al. (2007) indicate that higher fractal dimension is correlated with higher density in urban built-up areas. The results of the study imply that for a given urban context, the higher the value of fractal dimension, the denser and more homogeneous the built-up area will be. Higher fractal dimension also suggests the existence of larger urban mass, and hence, more urbanized urban areas.

Theoretical expectations imply a strong separation between fractal and density in the other direction from the one discussed above. As illustrated in Figure (2-8), areas with the same density can have different fractal dimensions. While both figures have the same density (64 black squares), the fractal dimension of (a) is more than that of (b). Thus, fractal dimension as an explanatory tool for density of the built-up area should be used with caution (Thomas et al., 2008).

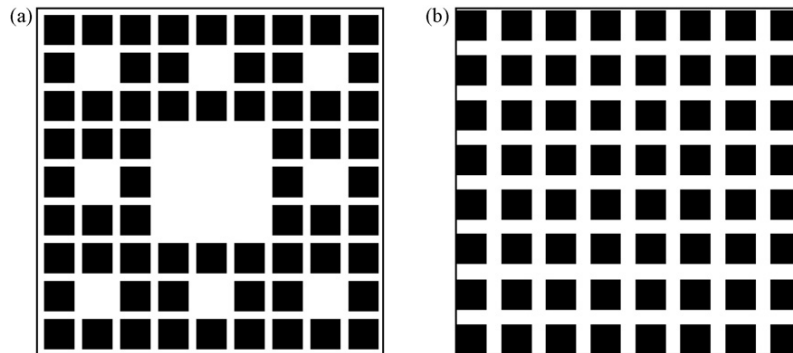


Figure (2-8): Illustration of two figures with the same density but different fractal dimension: $D(a)=1.89$, $D(b)=2.0$ (Retrieved from Thomas et al., (2008))

Development Stage, Housing type, Rent and Income

Fractal dimension has been proved to be useful to characterize the socio-economic properties of urban areas, such as average income and rent value of households. Keersmaecker et al. (2003) have studied the city of Brussels to explore whether fractal analysis can be used as a meaningful tool to infer intra-urban properties that are commonly used in urban planning and geography. For this purpose, the map of the city is divided into 25 equal windows, and for each window, the fractal dimension is calculated. Comparing results of all windows, the authors discuss that fractal dimension tells us more about the structure than does density.

They conclude that there is a strong correlation between fractal dimension and the stage of the development, dominant housing type, average rent and income value. As such, fractal dimension declines with distance from city center, similar to the development stage of cities. This is due to the fact that distance plays a key factor in in the internal structure of cities (Anas et al., 1998). As competition for shorter distances to city center is higher, cities grow from their center, and thus the stage of urbanization declines as distance from CBD increases. This process also influences residential location choice and housing type. Anas et al. describe that locations closer to CBD are usually filled with apartment buildings, inner suburbs with town houses, and outer suburbs with

detached and semi-detached houses. This also explains why the average rent and income value increase with fractal dimension.

Although Keersmaecker et al. (2003) have taken a big step forward toward understanding the role of fractal index in distinguishing the urban morphology, caution should be observed, as their results are limited to the case of Brussels, which has a specific planning history. So, fractal dimension needs to be coupled with an adequate model associated with the historical, economical and geographical background of the city.

Clustering Urban Areas Based on the Fractal Scaling Curve

Another example of analyzing the fractality of black and white maps of cities is a study by Thomas et al. (2010) of 49 cities in Europe based on the fractal dimension of their built-up area. In the first step, by comparing the shapes of the scaling curves, they have divided the cities into groups of similar shape. In the next step, they have analyzed the cities in each group based on their specific urbanization history and planning evolution. The results show that the spatial variation of urban texture provides interesting information about their intra-urban characteristics. More specifically, the

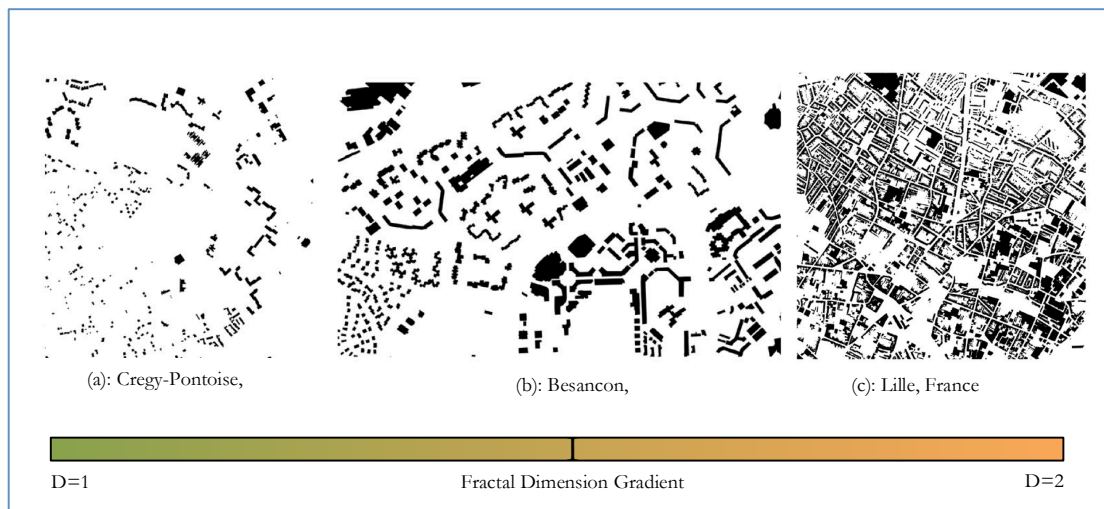


Figure (2-9): The correlation between fractal dimension and urban form texture. The colored bar represents fractal dimension (D) value ranging from 1 (linear) to 2 (planar) with corresponding examples of cities with D in that range. (Images retrieved from Thomas et. al., 2010)

clusters with higher average fractal dimension value (more than 1.7) are mostly the classic densely urbanized areas that have an organic structure (Figure (2-9-c)). These areas usually consist of dwelling in city centers mixed with few large buildings. Also, areas with Corbusian style design (Figure (2-9-b)), which are described as “tower in the park”, as well as newly planned towns in France with free-standing industrial or office buildings in a large area distant from each other cluster together based on shape of their scaling curves (Figure (2-9)-a).

This study clearly shows that there are links between the fractal dimension of urban form and the internal characteristics of urbanization history and planning styles. However, the fractal measure can only be used as a general indicator of internal urban structure rather than a guide to specific information.

Environmental Condition

Applications of fractal dimension have also been extended to study of the environmental condition of cities. Wang et al. (2011) indicate that fractal dimension may explain the environmental condition of a city in terms of balance between built-up and green space. They argue that as larger fractal dimension (D) means denser built-up areas and less green open space in urban fabric, it is also associated with a deterioration of environmental conditions. Using Lijiang city in China as case study, they analyzed fractal dimension using both the box-counting and the area-radius relationship methods. They showed that the areas with the highest fractal dimension are those where the percentage of green space is less than 12%. Accordingly, they suggest that further developments must stop filling the available spaces between built up areas, but rather, the city should focus on improving the quality and quantity of the green spaces in between.

Limitations in Applications

Although fractal dimensions have largely facilitated analysis in urban modeling, there exist several deficiencies to its application, especially associated with the growth processes. For instance,

as a very general indicator, fractal dimension is unable to provide accurate information in terms of cities' morphology. However, in order to be applicable, it needs to be coupled with other tools and measures that classify similar scaling curves together, as suggested by Thomas et al. (2010). Obviously, further investigation is required to empower fractal analysis for use in urban analysis.

2.4.2 Fractal Application in Visual Planning and Design

As fractals are primarily observed in natural objects -such as mountains, trees, snowflakes, and crystals- they are visually pleasing to human eyes (Spehar & Taylor, 2013). Therefore, fractal algorithms have been widely used to generate digital images that resemble natural features. Examples of this type of applications include synthetic natural sceneries with mountains and trees (Batty & Longley, 1994). Also, mathematical fractals such as the Mandelbrot Set and the Julia Set are considered as aesthetic illustrations (Batty & Longley, 1994).

The second class of fractal application in urban studies takes the reverse direction of creating beautiful images, that is, evaluating digital images. The role of fractal dimension in analyzing digital images has long been identified (Ruderman, 1997; Sato et al, 1996; Vudec, 1997; Yang and Purves, 2003), particularly, in the context of urban design. Cooper et al. (2010) have studied the relationship between human perception of beauty in the street vista in Witney, UK and the fractal dimension using the box-counting approach. The results of the study reveal that there exists a positive relationship between fractal dimension and the quality of the street vistas perceived by people walking in those streets.

Also, in a follow-up study comparing the effect of vegetation and fractal dimension on the perception of the visual quality of streets in Taiwan and UK cities, Cooper et al. (2013) show that, although both factors have positive effect on respondents' perception of beauty, the fractal dimension shows stronger correlation. They discuss that this correlation is the result of differences in scaling between scenes dominated by natural environment vs. those dominated by built features.

Thus, fractal dimension can be used to evaluate the visual quality of urban design projects to help achieving more attractive and pedestrian-friendly streets.

2.4.3 Fractal application in urban modeling

The third class of fractal applications aims to understand how cities grow, evolve and change spatially and non-spatially. As fractal geometry is the closest geometry to describe city form, scientists have attempted to understand the underlying mechanism that is common in natural and built systems that lead to emergent fractal patterns. This investigation has been made possible with computer simulations that iterate a function over the scope of time and space. Such urban modeling studies can be classified in three categories: statistical models, Cellular Automata (CA) models, and Agent-Based models (ABM). The application of fractals and scaling in the first two classes of models is more evident. Thus, I focus on reviewing relevant studies developing statistical and cellular automata models in the following sections.

Statistical models

Statistical models have widely been used to explore the patterns of urban form and dynamics in regard to fractal properties. For example, Batty et al. (2008) have studied the internal structure of cities by looking in to the size distribution of buildings. More specifically, they have explored how geometric properties of buildings scale as they grow in size and also with respect to the distance from the city center. In order to build a general context for their studies, they have investigated the scaling behavior of world's 200 highest buildings and compared it to London's, Tokyo's and New York's 200 highest buildings. Their analysis reveals a strong scaling relationship consistent in all four databases as shown in Figure (2-10) below. On the left, the distribution plot of the world's most populous cities is drawn next to the distribution of world's highest buildings. The comparison

reveals that the slope of the latter is more than the former, which indicates that there is more competition between people for urban units than between cities.

The comparison between distribution plots for cities on the right shows that New York has the steepest rank-size relationship and London has the flattest. However, there is log-normality evident in New York and Tokyo's databases, which suggests that more caution is required in approximating urban distributions by power-law. As discussed earlier, empirical fractals do not follow a power law perfectly due to functional or spatial constraints or measurement methods. For example, the way buildings' height is measured and the urban boundaries are defined affect the patterns of the rank-size distribution function to a considerable extent. The above preliminary analysis provides the necessary baseline for their main study by confirming the fact that, there is strong scaling relationship in geometric properties of buildings.

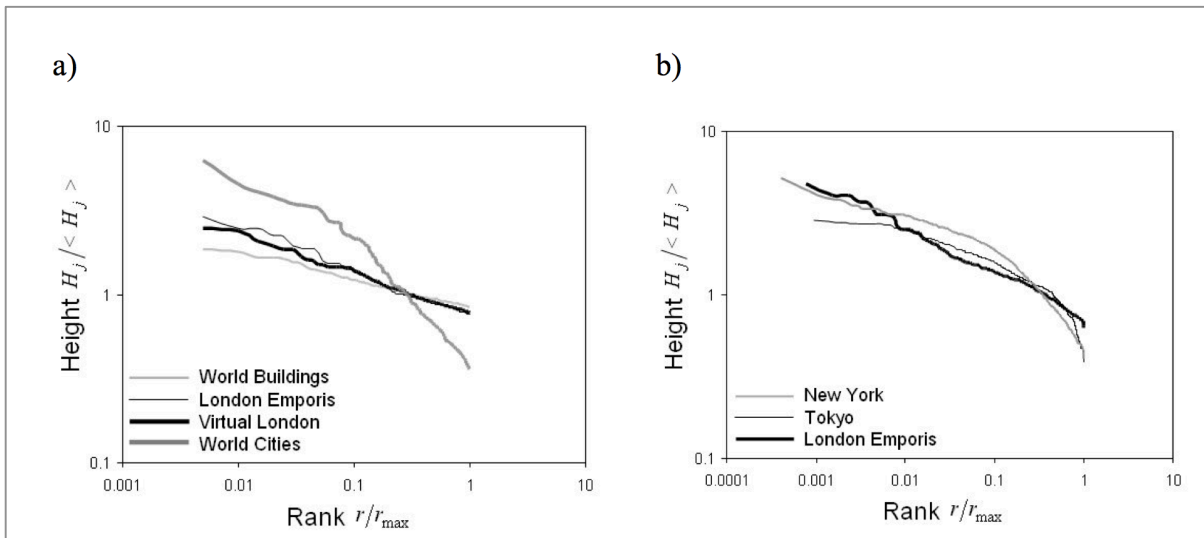


Figure (2-10): Initial analysis of building heights a) top 200 buildings by height in the world and London, and top 200 city populations, b) top building heights in New York, Tokyo and London (adopted from Batty et al., (2007)).

In the main part of their study, Batty et al. (2007), explore the scaling properties of London buildings based on their Euclidean geometric properties: perimeter, area, height and volume. The rank-size distribution graphs of all four databases reveal strong linearity along all scales. This is consistent with a power law distribution. Also, the same analysis with respect to nine land use

categories produced the same dramatic power-law patterns in log-log plots. The authors believe that the scaling pattern found in London buildings is the best among all other urban aspects such as roads and parcels.

The next step of their analysis of the behavior of each geometric property with respect to others indicates that as the buildings grow in size, their shapes change as well. More specifically, the area of buildings grows less than perimeter, as expected geometrically with square power of area compared to single power of perimeter. They hypothesize that this is due to the fact that as area grows, buildings try to maximize their surface area for lighting. This is also the case for the volume of the buildings with regard to area.

Lastly, Batty et al. (2007) have employed two-point correlation function to explore whether distribution of building locations in space is fractal. The analysis reveals that among the four geometric properties that are studied, only the height of the buildings is distributed in a fractal pattern.

Scaling patterns have also been studied for the distribution of parcels in cities. Fialkowsky and Bitner (2008) have investigated the distribution of parcel sizes based on Euclidean area in 33 different cities in US, Australia and Europe. They demonstrated that the log-log plots of parcel sizes in all of these cities fit a straight line and follow a generic power-law pattern. The behavior of plots with changes in radius of the area under study provides a promising method to distinguish the urbanization level in each area. They found that the distribution function of parcel sizes in the city core has a power law tail with exponent of 2, it follows a log-normal pattern in suburbs and a power-law with exponent of 1.1 in rural areas. The methods that are used to determine the exponent values are based on first, calculating the slope of the linear model fitted to the log-log plot and second, by using the maximum likelihood estimate. The former method is dependent on the binning of distribution data, while the later one is free from this uncertainty and is known as the best

method of fitting parameters of distribution functions. Notably, both methods have returned very similar values for power-law exponents.

The authors have referred to the existing literature to interpret these observed patterns in urban morphology. They suggest that geometric Brownian motion (GBM) can represent the governing mechanism for the transformation of rural areas to suburban areas, which give rise to lognormal distributions. GBM is a stochastic multiplicative process that accounts for both the split and merge of a parcel in rural to suburban transformation. The power law pattern in urban core can also be explained by random partitioning of the plane, which is used to model the distribution of human settlements in nations (Morgan & O'Sullivan 2009). Another simple model that can possibly explain the regularities is the model by Marsili and Zhang (1998), which includes interacting individuals who migrate and aggregate to form human settlements. Their model takes into account the tendency of individuals toward larger cities, but also their avoidance from the undesirable impacts of aggregation.

In general Fialkowsky and Bitner (2008) have contributed to finding very similar patterns in the distribution of parcel sizes in several cities in US and Australia. All of these cities have similar planning and formation history. However, the inclusion of only one old European city, Krakow, in the study is not sufficient to conclude that the observed pattern is generic and worldwide. The city of Krakow might be an exception to other European cities and does not also represent all medieval towns. Thus, I think it is required to extend this study to more cities in Europe and elsewhere with various size and planning history to generate confident results.

Cellular Automata and Fractals

Since Wolfram (1984) first demonstrated that CA models could generate fractal patterns, these models have attracted the attention of urban scientists to simulate natural dynamics of cities. Cellular Automata refers to computer simulations that model each land unit as a cell with a value

that describes the state of the land. As the model iterates, the state of the cells may change based on the transition function that rules the system, which take account the neighborhood relationships. This class of models is specifically suitable for modeling land-use dynamics, since locations can be explicitly modeled and each cell needs to have only one state at a time. CA models are also favorable for modeling neighborhood effect by taking the state of neighboring cells into account for transition formula (Batty and Longley, 1994).

For the first time, CA was used to link theory to empirical realism in urban studies by White and Engelen (1993). The authors have modeled the growth of a hypothetical city over 40 iterations with four different land use states: vacant, residential, commercial, and industrial. Using very simple transition rules and growth rates, they show that the simulated city grows with a realistic spatial distribution. In particular, the log-log size-frequency plot of commercial clusters has a linear structure, which suggests that the cluster sizes are distributed in a fractal pattern. Their results are in agreement with empirical studies on a set of US cities showing that 75% of cities have fractal pattern in their cluster-size frequency of commercial land uses. However, the question remains why the fractal structure emerges only within relatively limited regions with a specific set of parameters.

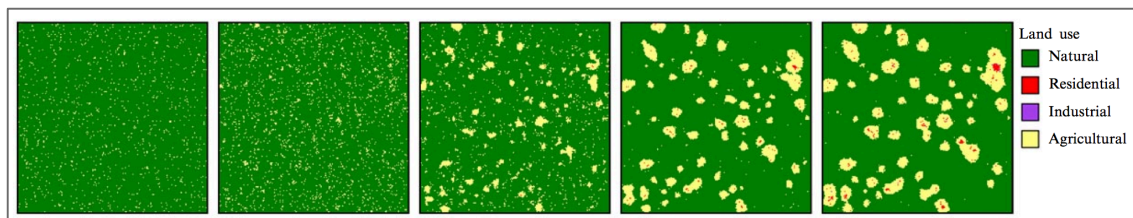


Figure (2-11): Time series representing land use distribution of a simulation for regular time intervals. (Retrieved from van Vliet, et. al., 2012)

Since the first step was made by the above study, CA continued to be favored for modeling and representing spatial patterns of cities (Chen et al., 2014). For example, it has been shown that supplementing CA with agent-level information can result in achieving more realistic urban patterns. In the study by van Vliet et al. (2012), the transition rules for cells representing land use are designed to change incrementally. As such, instead of changing suddenly from residential to commercial, for

instance, the land first changes from low-density residential to high-density residential and from there, to commercial or industrial. The model simulates an urban region with limited number of houses and jobs sparsely distributed in a model landscape. After 1000 time steps, settlement clusters emerge in the landscape as demonstrated in Figure (2-12).

The rank-size distribution of each land-use cluster, represented in the model, fits into a power-law distribution model very well. The result is aligned with the expected pattern for a system of cities and towns in a region as discussed by Cordoba (2008) and Gabaix (1999). The authors believe that the emerging pattern is the result of two counter-acting forces in the model dynamics: the neighborhood effect working as a centripetal force, and the diseconomy of scale and stochastic perturbation working as centrifugal forces.

The subject of both studies explained above is the system of several towns and settlements in a region looking at the size distribution of land-use clusters. However, the question remains: why does the internal distribution of buildings in a single city follow a fractal pattern and how can we model it? Chapter four is dedicated to exploring this gap and developing a hypothetical framework that explains why fractal patterns emerge in city scale distributions.

Chapter 3: Kitchener-Waterloo Case Study

In this chapter, I apply the rank-size fractal dimension calculation method that was discussed in Chapter 2 to the urban wards of Kitchener-Waterloo. This case study, although is not directly connected to the main contribution of this thesis, provides an insight into the application of fractal dimension as a measure of urban form. I selected Kitchener-Waterloo because, as a resident I am familiar with the urban context and can explore the connection between the values calculated for each urban district to the social, and spatial characteristics with more tangibility. First, I start with a small synthetic example and then proceed to the empirical study.

3.1 Synthetic Landscapes

For the purpose of demonstrating the method that is used in this chapter, I create a set of synthetic landscapes with distinct designs. The design variations are set to reflect the primary elements in the evolution of urban form including points of attraction (assumed as generator seed) and main transportation lines (assumed as axis). The four landscapes designed for this purpose are identical in their overall shape and area as well as the density of occupied space by their elements. The same idea is repeated in all four landscapes to fill the space: In each iteration, the largest possible circle that can fit in its available space is generated. However, the initial condition varies by the number and form of the initial seeds or axis (I interpret the initial seeds as the urban centers and the axis as the main transportation routes). Figure (3-1) shows the initial pattern-generator elements of each landscape. In landscape A1, the initial element is set to the minimum, one central business district with no transportation route. The outcome pattern generated with the idea of filling the available space with the largest possible circle is demonstrated in Figure (3-2).

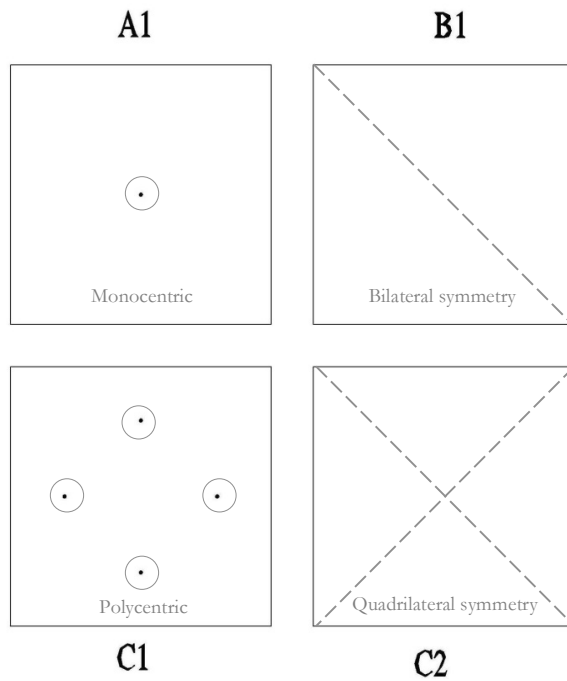


Figure (3-1): Synthetic landscapes' pattern-generator elements.

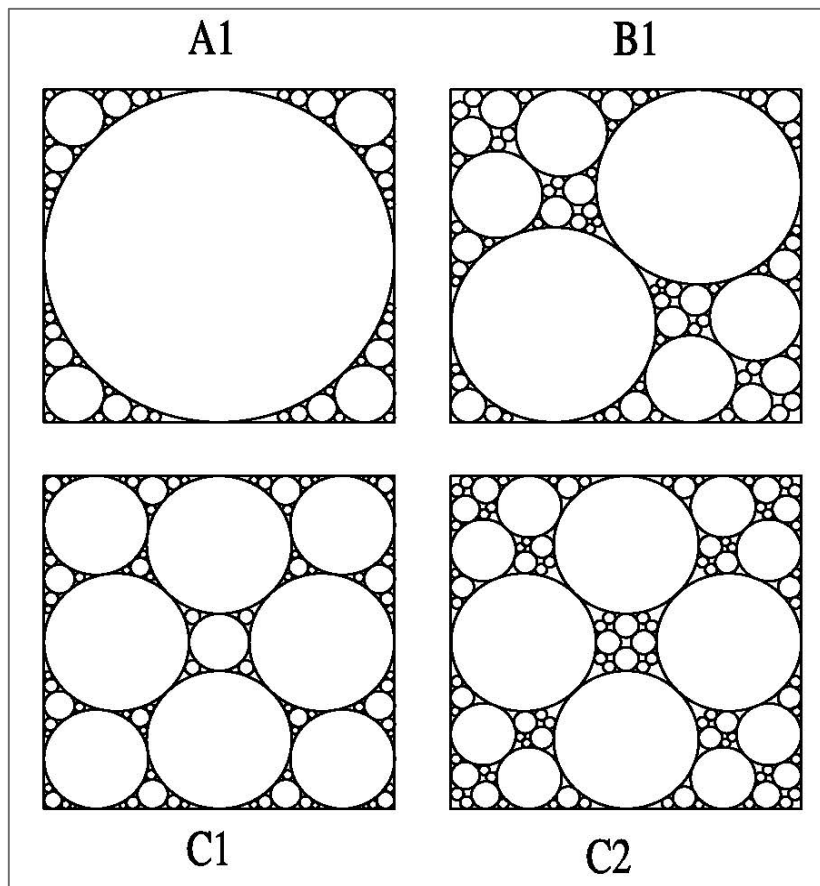


Figure (3-2): Synthetic landscapes demonstrating different outcome based on various initial conditions. (These landscapes are generated manually in Auto CAD using the *three-tangent circle* command)

In landscape C1, the initial elements are set to represent a polycentric city with four influential city centers but no transportation route. The same process as in A1 is repeated to fill the spaces. A very different pattern is yielded with tighter range of size variable as demonstrated in Figure (3-2).

Landscapes B1 and C2 are intend to represent main transportation routes' effects on generating patterns in urban form². In B1, the space is divided into two equal regions leading to automatic creation of urban centers in both sides of the route. Similarly, in landscape C2, two perpendicular transportation routes are modeled. The outcome pattern of this design is demonstrated in Figure (3-2)-C2, which is very similar to C1. In both cases, a polycentric pattern is generated with four influential cores. However, C1 allows for formation of broader variation of sizes compared to C2. More discussion is provided in the next section using distribution graphs for each landscape designs.

Figure (3-3) indicates log-log graphs of the frequency-size distribution for the synthetic landscapes. The overall patterns in all of the graphs are linear in a log-log graph, which reveal power law regularity. It implies that each of the landscapes has many small-size components, some middle-size and very few large-size components. However, as the number of circles in the synthetic landscapes is too small, they do not provide sufficient number of input data for a valid regression analysis. If it were possible to iterate the synthetic landscape generation process more in an unbounded space, it would help to have a more reliable regression analysis.

² This assumption is based on a two-dimensional space such as a city, where the construction of a major transportation route such as a boulevard or highway, divides the space into two districts that cannot have easy access to each other as before. Such transportation route separates the urban development styles and functional connectivity to some extent.

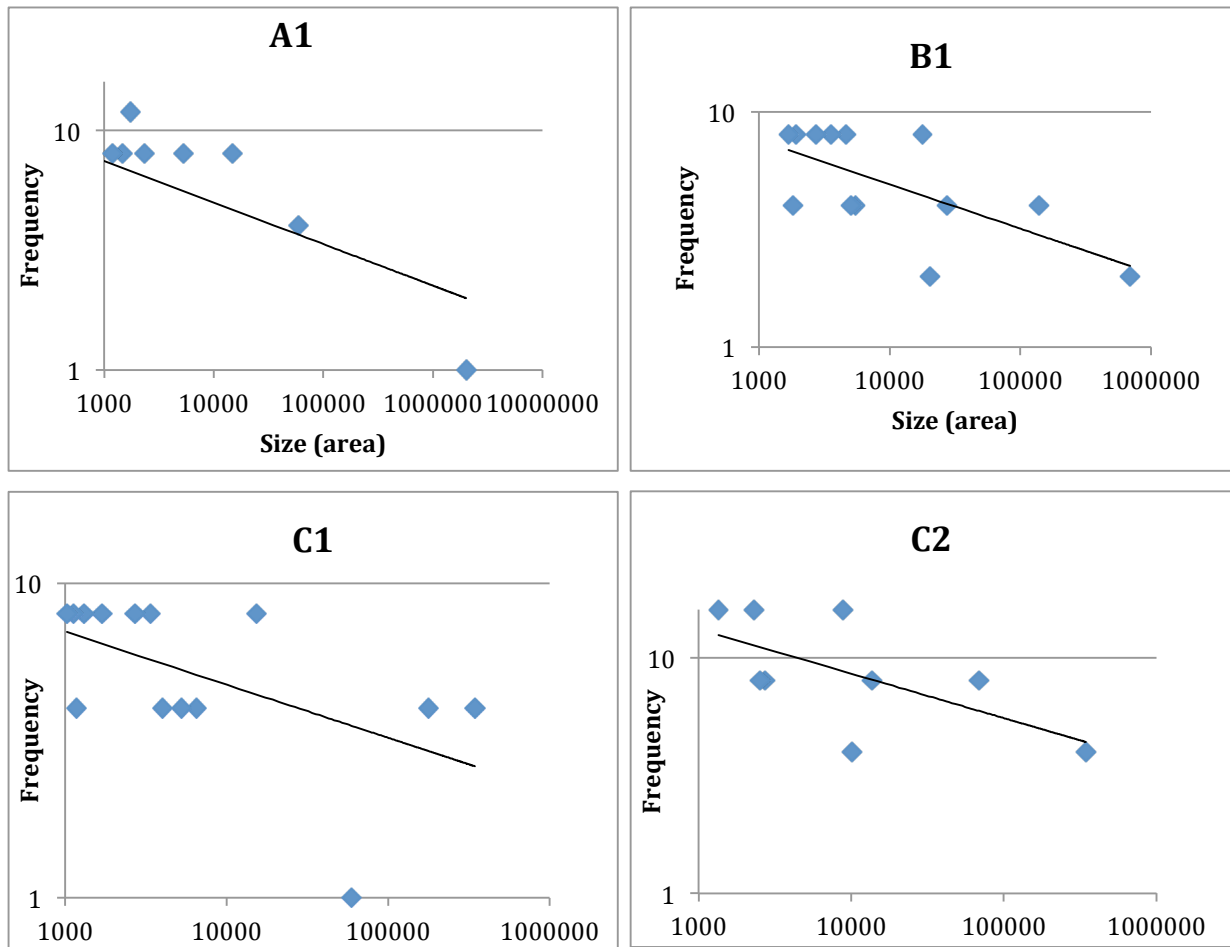


Figure (3-3): Graphs representing log-log power distribution of element sizes in each synthetic landscape. X-axis represents the size of elements in landscape, while Y-axis is the number of elements in that size.

| | A1 | B1 | C1 | C2 |
|---------------------------|------|------|------|------|
| Fratl Dimension (D_f) | 1.64 | 1.81 | 1.83 | 1.81 |
| R^2 | 0.65 | 0.43 | 0.31 | 0.39 |
| Number of observations | 105 | 72 | 81 | 88 |
| Number of iterations | 9 | 14 | 15 | 10 |

Table (3-1): power law properties of four synthetic landscapes provided in

Table (3-1) contains the regression analysis results for the landscapes. The slope of the regression line is the power factor in Equation (2-1), which shows how the frequency of each component scales with its size. The power factor equals $D_f - E$, where D_f is the fractal dimension and E is the Euclidian dimension of area ($E=2$) (Batty & Longley, 1994). Therefore, the slope of the regression line equals to $D_f - 2$. In A1 for instance, D_f equals to 1.64, which is significantly smaller than other landscapes. This can be explained by the lack of variation of size among circles that is imposed by the dominance of the large circle taking up the majority of space.

Landscapes B1 and C2 have the same fractal dimension of 1.81. This result strongly agrees with the basic definition of fractal objects regarding self-similarity. Comparing the two landscapes, it can be noticed that the same shape is repeated in both. B1 is made up of two similar parts or modules, and C2 is made up of four modules that are the same as the modules of B1. Although the scale of these modules in B1 is larger than C2, and the modules are positioned differently, the shapes of the modules are exactly identical, which explains why both landscapes reveal the same fractal dimension. As discussed in Chapter 2, fractal dimension is independent from scale and the unit of measurement.

Landscape C1 has the largest fractal dimension among all, which is equal to 1.83. The difference between C1 and C2 is the existence of transportation routes. Although in C2, the perpendicular axes have divided the landscape into four equal regions creating four urban centers as in C1 (notice that identical components have appeared in the first iteration in C1 and C2), in the next iterations the components are strictly ruled by the routes and cannot be distributed as freely in the space available to them as in C1. Therefore, in C1 components are scaled down by a smaller exponent, allowing larger number of iterations and broader size variation to take place.

As demonstrated in Table (3-1), the coefficient of determination (R^2) for D_f values calculated from the regression analysis does not show a good fit. This can be due to two sources of error: first,

the number of input data from these experiments is very small as the minimum value of size variable is set to 1000. That means I have not shown iteration results that generate circles smaller than the 1000 unit area. This would not cause a problem in the case of perfect fractal generation. However, there exists no intention to form a fractal object in the process of generating the current landscapes. The second source of error is due to the way the experiments are designed. For the purpose of simplicity in drawing and comparison, the scale and geometry is designed to be as simple as possible. This means that all landscapes are drawn in rigid square boundaries of a 1600 to 1600 pixel. Thus, it is not expected to see ideal results in spite of these limitations.

By performing this small-scale experiment, I came to infer that fractal dimension analysis using the power law distribution model is a valid method that can distinguish similar spatial patterns. Among landscape elements, the more the size varies between two consecutive size scales, the lower the fractal dimension is and the less the system fills the space available to it. Also, it can be derived from the experiment that spatial constraints like boundaries and transportation lead to smaller fractal dimension in general.

I intend to extend the scope of this experiment in a larger size landscape with more iterations to have sufficient number of observations for better regression analysis in my future work. In the next section, the method applied in the synthetic landscapes is used to analyze scaling in the distribution of Kitchener-Waterloo urban morphology.

3.2 Kitchener-Waterloo case study

In this section, I analyze the complexity of Kitchener-Waterloo urban forms in terms of fractal dimension of size distributions of physical elements both in aggregate and local scales.

3.2.1 Maps and Data

The morphology of physical urban elements including buildings' footprints, roads map and parcels map of Kitchener and Waterloo cities form the dataset for this analysis. The data is in vector format created by the Region of Waterloo for 2009. Although there are more recent data available for some data types, for the purpose of maintaining consistency between buildings, roads and parcel layers, the data from the same year is selected for all layers. Unreasonably large and small data in each layer are removed to avoid artifacts. Examples of these data include shelters, doghouses, parking structures, and urban installations.

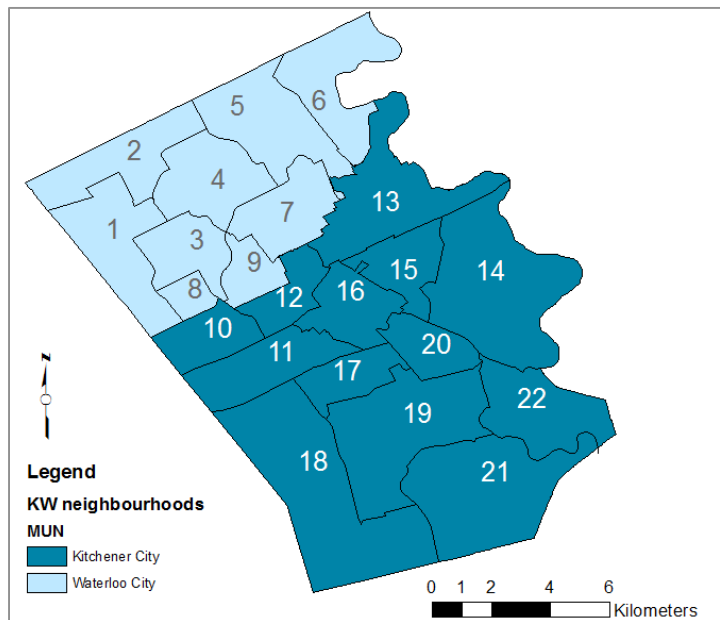


Figure (3-4): Kitchener-Waterloo urban wards (numbers indicating Neighborhood codes)

There were two main reasons for selecting Kitchener-Waterloo as the case study. First, for the interpretation purposes I need to compare the analysis results to the social and historical characteristics of each ward. Thus, accessibility to the area and having background knowledge about the planning history of the cities plays an important role. Second, Kitchener-Waterloo provides a small-scale case study with limited number of urban wards varying from old downtown district to

new suburban developments. This experiment paves the way for larger-scale studies, which include various regions for better calibration.

Figure (3-4) displays the wards within each city. Waterloo is composed of 9 wards, but only 7 of them are eligible for the purpose of this research. The two wards that are excluded are barely developed and mostly consist of agricultural lands. Kitchener has 13 wards labeled from 10 to 22 as listed in Table (3-2).

| NCODE | Neighbourhood name |
|--------------|-------------------------------------|
| 1 | West Waterloo |
| 2 | Lakeshore North/Conservation |
| 3 | Beechwood |
| 4 | Columbia/Lakeshore |
| 5 | Lincoln/Dearborn |
| 6 | Eastbridge/Lexington |
| 7 | Central Waterloo |
| 8 | Westvale |
| 9 | Westmount |
| 10 | Highland West |
| 11 | Forest Heights/Forest Hill/Lakeside |
| 12 | Victoria Hills/Cherry Hill/ KW Hosp |
| 13 | Bridgeport/Breithaupt/Mt Hope |
| 14 | Grand River/Stanely Park/Chicopee |
| 15 | Frederick/Rosemount/Auditorium |
| 16 | Downtown Kitchener and Area |
| 17 | Alpine/Laurentian |
| 18 | Southwest Kitchener |
| 19 | Country Hills |
| 20 | Vanier/Rockway |
| 21 | Doon/Pioneer Park |
| 22 | Hidden Valley/Pioneer Tower |

Table (3-2): Neighborhood names. NCODEs 1-9 are in Waterloo and NCODs 10-22 are in Kitchener

3.2.2 City-scale scaling analysis

In this section I have analyzed the three layers of data for power law distribution analysis for the whole city and for neighborhoods respectively. The purpose of this analysis is to provide a primary understanding of the distribution function of elements in each layer. If they exhibit a power-law distribution (with R^2 greater than 0.95), I will conclude that the distribution has a scaling behavior and that the fractal dimension can be calculated.

Table (3-3) summarizes the results from the regression analysis of roads' length, parcels' area and buildings' size distributions in Kitchener and Waterloo extracted from graphs in Figure (3-5, 3-6 & 3-7). The equations used for this purpose are provided by Batty (1994) as:

$$L(r) = N(r)r = ar^{1-D}$$

For length distributions where r is the scale, $N(r)$ is the number of elements in scale r , and $L(r)$ is the length for scale r . The equation is as follows for area distribution:

$$A(r) = L(r)r = ar^{2-D}$$

Figure (3-5) shows the log-log graph of frequency of roads by their length for Kitchener in left and Waterloo in right. The results from regression analysis indicate that the power law model explains at least 96% of the variations in the roads data in both cities as shown in Table (3-3).

| | Roads FD | R² | Parcels FD | R² | Buildings FD | R² |
|------------------|-----------------|----------------------|-------------------|----------------------|---------------------|----------------------|
| Waterloo | 1.75 | 0.96 | 1.49 | 0.91 | 2.34 | 0.97 |
| Kitchener | 1.74 | 0.98 | 3.80 | 0.99 | 2.51 | 0.94 |

Table (3-3): Fractal dimesnions for roads, parcels, and buildings in KW

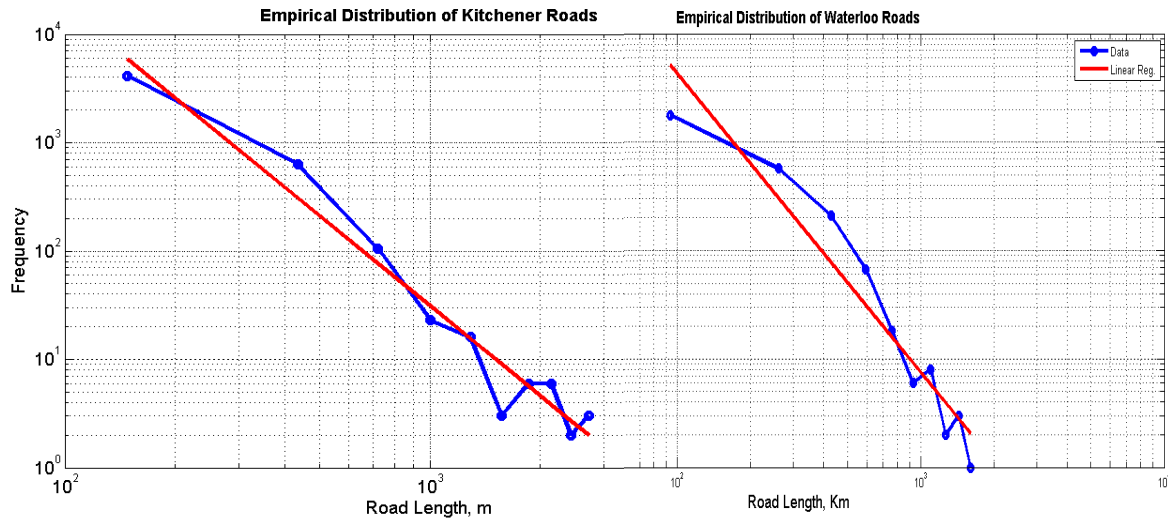


Figure (3-5): Log-Log graph of road length frequency in Kitchener (left) and Waterloo (right)

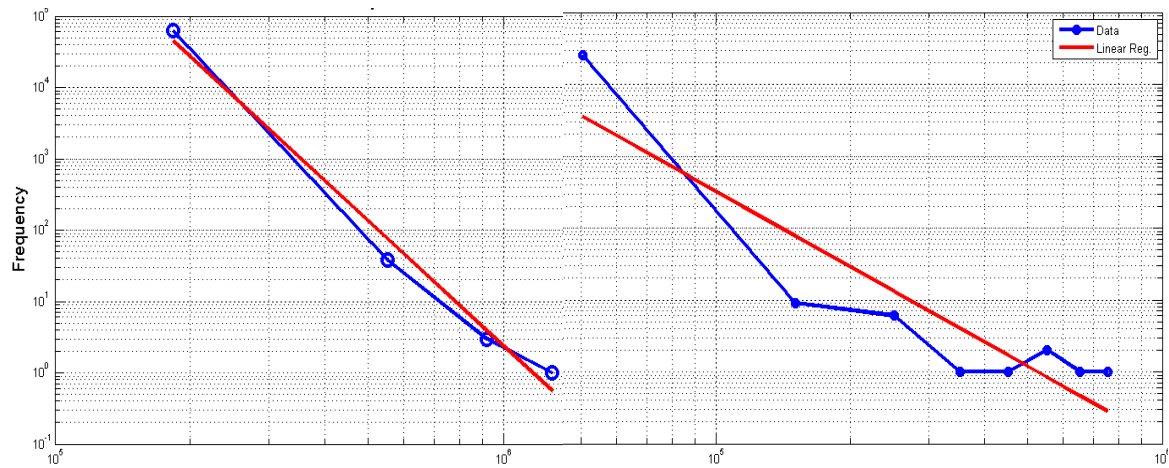


Figure (3-6): Log-Log graph of parcel area frequency in Kitchener (left) and Waterloo (right)

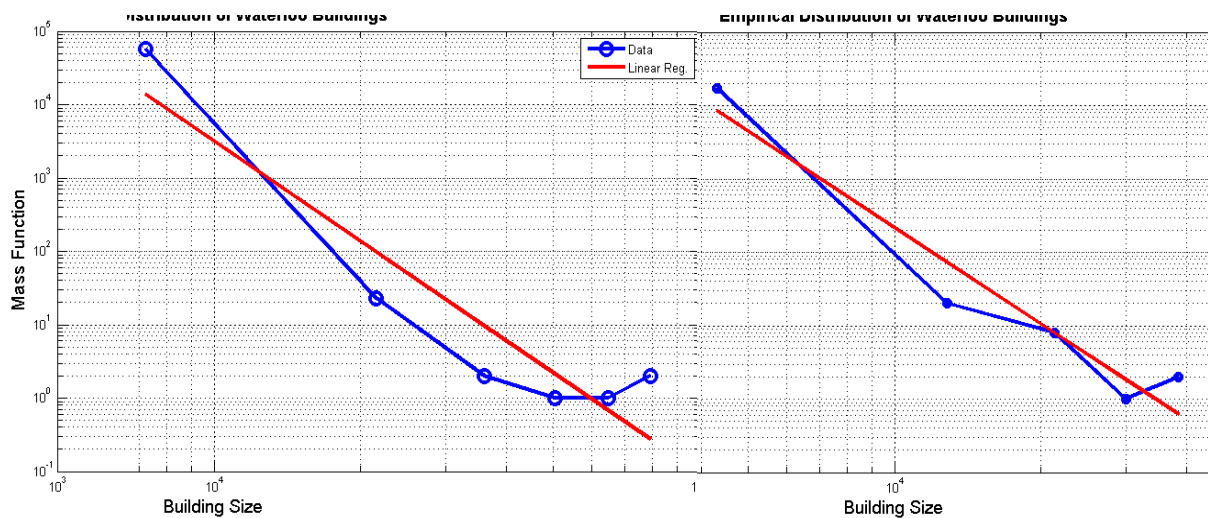


Figure (3-7): Log-log graphs of building area frequency in Kitchener (left) and Waterloo (right)

The convex behavior of the graph for middle and small ranges can be due to the fact that in real world the sizes of roads do not fall below a certain meaningful value. Also, the irregular bends at the tails reflect drops in the frequency of very long road and highways, as small regions such as Kitchener-Waterloo do not have variety of large-scale components. This analysis reveals the imperfect nature of empirical data for small-scale analysis that do not exhibit an ideal frequency for large components.

Unlike roads, the distribution of parcels shown in Figure (3-6) exhibits a concave curve, revealing the high frequency of very small and very large parcels compared to middle ranges. In Waterloo, the deviation is more significant. This can be due to the concentration of technological institutions and huge industrial land uses in the city of Waterloo. The rapid development of industrial and institutional uses in Waterloo has limited the natural evolution of the urban fabric, and thus a concave curve is observed.

In Figure (3-7), the frequency of building areas is presented in log-log graphs. The same general pattern is evident for buildings as in parcels. Higher-than-expected frequencies of very large and very small buildings are manifested particularly in Kitchener. This is due to the fact that Kitchener developed earlier than Waterloo, mainly along Victoria Street and King Street, where a concentration of factories and industrial uses exist. However, buildings are subject to change and evolve easier and faster than parcels. This can explain the considerable difference between parcels and buildings graphs for Kitchener.

3.2.3 Intra-urban Scaling Analysis

In this section the same analyses as in the previous section have been applied to the distribution of roads, parcels and buildings in each neighborhood. In Table (3-4) and (3-5), the neighborhoods are represented by their ID codes and names. Three sets of information for each neighborhood are reported including: number of observation of roads, parcels, or buildings in that

neighborhood, R-squared value showing how well the distribution fits to a power law, and D, the fractal dimensions, which are only valid for neighborhoods with a power law distribution. Neighborhoods with R-squared of more than 95% are highlighted as dark green in the tables and are considered as power law, those with R-squared between 93% and 95% are marked as light green. The corresponding neighborhoods are rendered in city maps, with the same color-coding (Figure (3-8) and (3-9)). Further representation of neighborhood distributions is provided in detailed graphs in Appendix II.

Table (3-4): Fractal dimension of parcels' size distribution in Kitchener-Waterloo

| NCODE | D of parcels | R² | Number of observations | Neighborhood names |
|--------------|---------------------|----------------------|-------------------------------|-------------------------------------|
| 1 | -0.72 | 0.84 | 3452 | West Waterloo |
| 2 | -0.60 | 0.88 | 1137 | Lakeshore North/Conservation |
| 3 | -0.75 | 0.94 | 2703 | Beechwood |
| 4 | -0.11 | 0.89 | 640 | Columbia/Lakeshore |
| 5 | -0.58 | 0.94 | 2617 | Lincoln/Dearborn |
| 6 | -0.81 | 0.96 | 3361 | Eastbridge/Lexington |
| 7 | -0.54 | 0.96 | 3285 | Central Waterloo |
| 10 | -0.46 | 0.81 | 2904 | Highland West |
| 11 | -0.97 | 0.90 | 6858 | Forest Heights/Forest Hill/Lakeside |
| 12 | -0.77 | 0.90 | 2908 | Victoria Hills/Cherry Hill/ KW Hosp |
| 13 | -0.90 | 0.97 | 4505 | Bridgeport/Breithaupt/Mt Hope |
| 14 | -1.17 | 0.93 | 9523 | Grand River/Stanelly Park/Chicopee |
| 15 | -0.82 | 0.93 | 4654 | Frederick/Rosemount/Auditorium |
| 16 | -0.71 | 0.92 | 4930 | Downtown Kitchener and Area |
| 17 | -0.46 | 0.91 | 2846 | Alpine/Laurentian |
| 18 | -0.43 | 0.86 | 3957 | Southwest Kitchener |
| 19 | -0.72 | 0.88 | 4094 | Country Hills |
| 20 | -0.58 | 0.86 | 2412 | Vanier/Rockway |
| 21 | -0.83 | 0.89 | 4855 | Doon/Pioneer Park |
| 22 | -0.30 | 0.94 | 991 | Hidden Valley/Pioneer Tower |

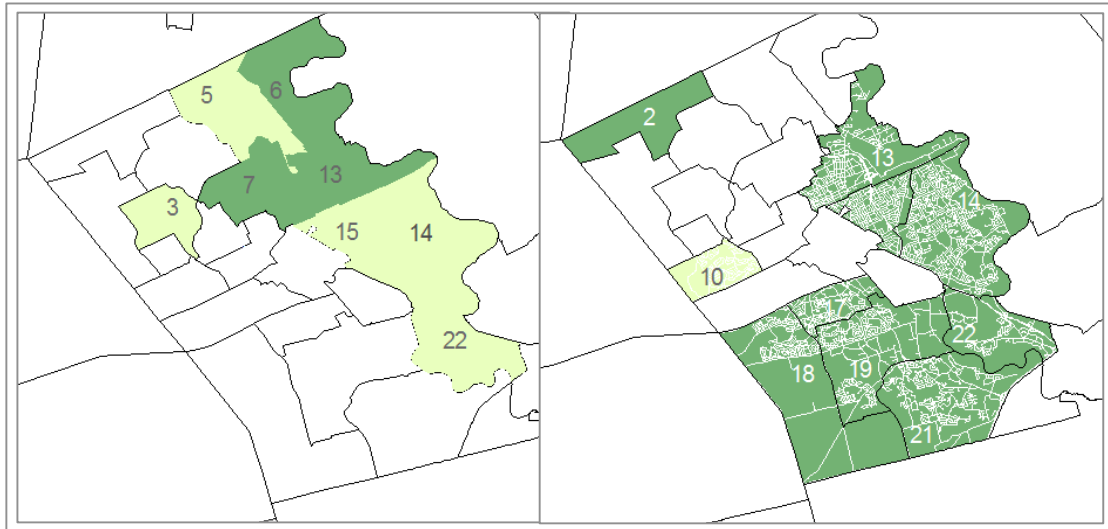


Figure (3-8): Neighborhoods with power-law distribution for parcels (left), roads (right). Dark green represents wards with goodness of fit of higher than 0.95, and light green represents goodness of fit of between 0.93 and 0.95 to the power law model

| NCODE | D of roads | R ² | Number of observations | Neighborhood names |
|-------|------------|----------------|------------------------|-------------------------------------|
| 1 | -0.5217 | 0.90 | 291 | West Waterloo |
| 2 | -1.0893 | 0.96 | 307 | Lakeshore North/Conservation |
| 3 | -1.1346 | 0.93 | 421 | Beechwood |
| 4 | -1.1063 | 0.92 | 449 | Columbia/Lakeshore |
| 5 | -0.5633 | 0.91 | 382 | Lincoln/Dearborn |
| 6 | -0.9743 | 0.93 | 339 | Eastbridge/Lexington |
| 7 | -1.4342 | 0.92 | 465 | Central Waterloo |
| 10 | -0.5386 | 0.95 | 170 | Highland West |
| 11 | -0.9898 | 0.92 | 432 | Forest Heights/Forest Hill/Lakeside |
| 12 | -0.4679 | 0.91 | 205 | Victoria Hills/Cherry Hill/ KW Hosp |
| 13 | -1.3333 | 0.97 | 505 | Bridgeport/Breithaupt/Mt Hope |
| 14 | -1.4321 | 0.97 | 847 | Grand River/Stanely Park/Chicopee |
| 15 | -1.4127 | 0.95 | 462 | Frederick/Rosemount/ Auditorium |
| 16 | -1.2972 | 0.90 | 637 | Downtown Kitchener and Area |
| 17 | -0.7869 | 0.98 | 213 | Alpine/Laurentian |
| 18 | -0.6202 | 0.96 | 237 | Southwest Kitchener |
| 19 | -1.0333 | 0.97 | 375 | Country Hills |
| 20 | -0.9387 | 0.91 | 228 | Vanier/Rockway |
| 21 | -1.2566 | 0.98 | 436 | Doon/Pioneer Park |
| 22 | -0.7058 | 0.95 | 185 | Hidden Valley/Pioneer Tower |

Table (3-5): Fractal dimension of roads' length distributions in Kitchener-Waterloo

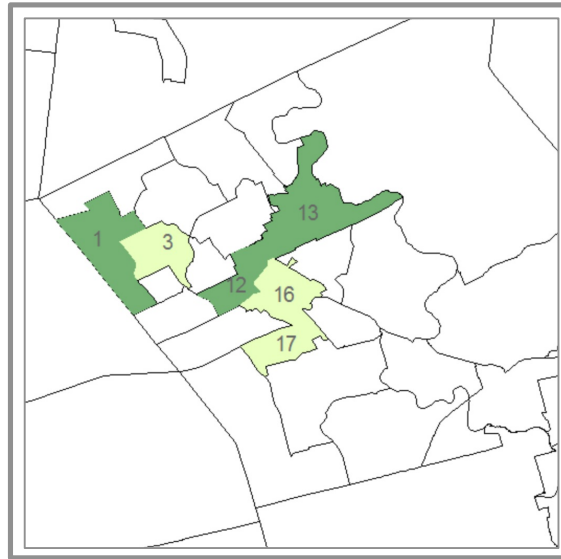


Figure (3-9): Neighborhoods with power-law distributed buildings. Dark green represents wards with goodness of fit of higher than 0.95, and light green represents wards with goodness of fit between 0.93 and 0.95.

| NCODE | D of buildings | R ² | Number of observations | Neighborhood names |
|-------|----------------|----------------|------------------------|-------------------------------------|
| 1 | -0.8153 | 0.96 | 3743 | West Waterloo |
| 2 | -0.5408 | 0.91 | 2166 | Lakeshore North/Conservation |
| 3 | -0.6571 | 0.95 | 4080 | Beechwood |
| 4 | -0.7206 | 0.84 | 3766 | Columbia/Lakeshore |
| 5 | -0.8216 | 0.90 | 4695 | Lincoln/Dearborn |
| 6 | -0.4781 | 0.86 | 3441 | Eastbridge/Lexington |
| 7 | -0.614 | 0.92 | 3348 | Central Waterloo |
| 10 | -0.5736 | 0.91 | 3323 | Highland West |
| 11 | -1.0199 | 0.90 | 7081 | Forest Heights/Forest Hill/Lakeside |
| 12 | -0.6346 | 0.97 | 2990 | Victoria Hills/Cherry Hill/ KW Hosp |
| 13 | -0.7786 | 0.95 | 5042 | Bridgeport/Breithaupt/Mt Hope |
| 14 | -0.8447 | 0.92 | 10981 | Grand River/Stanelly Park/Chicopee |
| 15 | -0.6716 | 0.88 | 4926 | Frederick/Rosemount/Auditorium |
| 16 | -1.0636 | 0.93 | 5688 | Downtown Kitchener and Area |
| 17 | -0.6303 | 0.93 | 2899 | Alpine/Laurentian |
| 18 | -0.3771 | 0.91 | 4589 | Southwest Kitchener |
| 19 | -0.3226 | 0.89 | 4847 | Country Hills |
| 20 | -0.6338 | 0.89 | 2498 | Vanier/Rockway |
| 21 | -0.9993 | 0.96 | 5179 | Doon/Pioneer Park |
| 22 | -0.2035 | 0.87 | 1325 | Hidden Valley/Pioneer Tower |

Table (3-6): Fractal dimension of buildings' size distributions in Kitchener-Waterloo

3.2.4 Discussion and Conclusion

This chapter provided an empirical study of scaling behavior in city and neighborhood scale. The study is conducted in city of Kitchener-Waterloo as a whole and in individual urban wards. The analysis looks at how the frequency of buildings, roads and parcels vary across scale. In the city-scale, Kitchener exhibits a better fit to the power law curve compared to Waterloo, particularly in the parcels' size distribution. This can be due to the longer history of development and larger number of data points in Kitchener that helps us to verify the analysis. The best fit to power law is for Kitchener parcels' data, which unlike other layers include enough small size parcels as well as an adequate number of large size parcels. However, the fractal dimension of Kitchener buildings is higher than expected due to the existence of higher number small-size buildings in Kitchener compared to Waterloo.

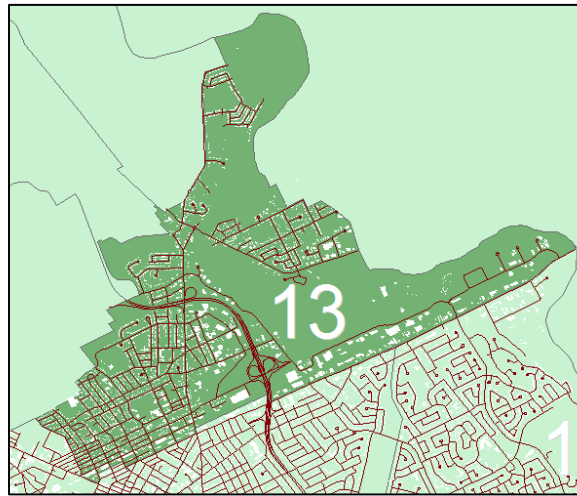


Figure (3-10): Bridgeport Neighborhood in Kitchener with roads and building footprints

For small-scale analysis, 8 out of 13 Kitchener neighborhoods fit a power law distribution for their road length with R-squared of at least %95. As shown in Figure (3-8)-right, these are all neighborhoods that contain large road segments such as highways. The reason is that the existence

of large-scale components (highways in this case) has made a broad enough variety of lengths to support scaling behavior.

For parcel layer analysis as shown in Figure (3-8)-left, the best-fitted neighborhoods are mainly concentrated in the northern border of Kitchener and central Waterloo. Best-fitted neighborhoods for building area distribution compose an interesting pattern, illustrated in Figure (3-9); neighborhoods that are close to Kitchener downtown and uptown Waterloo and are located along the King Street axis are highlighted. They include mainly the small-scale commercial and institutional parcels as well as small to mid-range residential buildings. They also contain few very large buildings such as hospitals, university buildings, big box stores and so on. The broad variety of sizes in these neighborhoods has made them eligible to have fractal properties.

Overall, only one neighborhood has survived to be a good fit to the power law distribution model through all data layers (buildings, parcels and roads), and that is the 'Bridgeport neighborhood' in eastern Kitchener with NCODE 13. As demonstrated in Figure (3-10), this neighborhood contains very large segments of road belonging to the Conestoga PKWY highway, as well as many short length roads in residential areas in its western parts. As for parcels and buildings' footprints, there are very large commercial-use parcels and buildings along Victoria Street and near the highway, as well as very small buildings in residential areas. This result shows that fractal properties of urban form are associated with mixed-use developments and settlement and aggregation history. As such, urban areas with variety of land uses and building sizes that has long history of development are more likely to have fractal properties.

Consequently, fractal analysis of intra-urban forms using power law distribution method provides a valuable tool to characterize urban neighborhoods in terms of the variation of the size of elements. However, this method needs to be complemented with measurements of spatial allocation of urban built up components to be able to estimate a fractal object.

Chapter 4: Model Framework

In Chapter (1), I developed a hypothesis that proposes a theoretical explanation for the similar fractal properties in the social and spatial facets of cities. The hypothesis sketches a new description for the process of urban growth that includes both social and spatial evolution. The hypothesis suggests that the fractal pattern in the urban physical form is originated from the allocation of power law- structured social groups, which have in turn emerged from an aggregation process. This chapter is dedicated to demonstrate the method that is employed to examine the presented hypothesis.

4.1 Goal of Modeling

As a preliminary step in testing my hypothesis, I adopt a theoretical explanatory model. Due to the advancement of computer simulations in the past few decades, it is possible to test hypotheses with computer models and experiment with several scenarios by changing model parameters fast and flexibly. I intend to use computer simulation to model the growth of a typical town from a single seed in space to a large urban landscape. The goal is to test whether the proposed aggregation and allocation process can generate realistic patterns in the outcome landscape that resemble fractals. For this purpose, I designed an agent-based model of a city with growing population who interact with each other and form groups and buildings, respectively. The model is composed of three main processes including population growth and allocation, aggregation of population into groups, and settlement and building allocation as shown in Figure (4-1) below. For each agent, these three processes are sequenced interdependently.

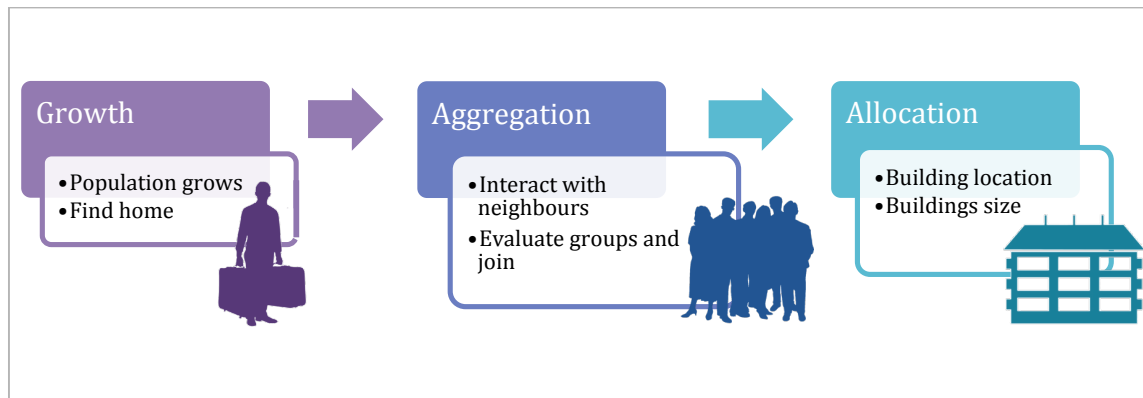


Figure (4-1): Model's key elements: growth process, aggregation process, and allocation process.

The first process represents the growth of the population based on the growth rate parameter and the allocation of newcomers to free lands near city center. The second process accounts for the aggregation mechanism in which individuals interact with each other and form groups with various size and location. This process forms the demand for the next step, which is allocation of a building for the group's activity. The third process is responsible for supplying the group's demand with a building that has the required size and location. This step takes into account spatial constraints such as maintaining the minimum distance to group members and also competition for space. More details on the model processes are provided in Section 4.3, the model design.

4.2 Agent Based Models

The best way to model such non-equilibrium multi-level, bottom up processes is to employ an agent-based model. Agent-Based Models (ABM) are a class of computational models that consists of autonomous agents who interact with each other and the environment (Railsback et al. 2012) and are widely used to model social and economic systems (Farmer & Foley, 2009). Agents are programmed explicitly to represent real people and firms with defined strategies and behaviors in regard to their environment.

There are three main features that made ABM the best choice for this study: ability to model complex systems, interaction between simple actors who can move, and emergent macro-scale

patterns. The only rules in the model are the micro-scale behaviors of the agents that govern their decision-making process and interactions. It is the iteration of these simple rules that leads to the emergence of macro scale patterns, either in the distribution or in the configuration of spatial elements of the model outcome. The model is complex because the decision of each agent has influence on all other agents and the environment. This makes the system path-dependent and behaviorally unpredictable (Batty, 2007). Path-dependency refers to the patterns in systems that are very sensitive to slight differences the process or initial conditions. It is the result of negative or positive feedback in the system and can lead to unpredictable behaviors (Brown et al., 2005). As a result, for complex systems, an analytical model that represents the system cannot be solved and its solution be analyzed. Thus, an agent-based model is a reasonable tool to experiment with model of complex phenomena.

Another advantage of any computer model of a city is that its parameters can be varied and previewed to explore the effect of such changes on the resulting spatial form. In this study, I investigate the effect of variations of overall model parameters including network size, transportation cost, growth rate, and activity rate of agents on the emergent structure of the model. These experiments are discussed in more details in the next sections.

4.2.1 Netlogo[®]

There are several agent-based modeling platforms available with different capabilities and limitations. One of the most user-friendly and widespread platforms is Netlogo[®] (Wilensky, 1999), which is employed in this study. Netlogo is an open source multi-agent programmable modeling environment that is Java-based. It has spatial representation that enables users to explore spatial patterns that emerge from interaction of interdependent agents. The especial feature of Netlogo is that it is user-friendly and does not require advanced programming skills. This makes the

communication of the model considerably easier than conventional platforms. It provides the ability to change parameters on the fly and preview the results in the outcome landscape.

As Netlogo is cell-based, vector-based representations are not conveniently implemented. Therefore, for landscape representation of the model, I used Repast[®] (North et al. 2013) which is a more advanced open source agent-based platform with GIS capabilities. In the first step the model is run in Netlogo and the location and size of each building is defined in the landscape. Then, in the second step, the resulting landscape is transferred to Repast[®] and based on a weighted Voronoi algorithm, parcel representations are made. For this purpose, Repast[®] treats the building locations as the centers of polygons (parcels) and the building sizes as their weight. The boundaries are then drawn such that the area allocated to each polygon is proportional to its weight as follows: $A_i/A_j = s_i/s_j$; where, A_i is the area of polygon i and s_i is the weight or size of building i . In other words, if 0.1% of the total model population use building i , then the area of polygon (parcel) i of the Voronoi map will be 0.1% of total settlement area. It is important to note that landscape representations in this model are very abstract and do not include transportation, and many other urban land-uses.

4.3 Model design

The model is designed to describe a process by which a new settlement might develop in a previously unsettled landscape. Suppose a central point in a plain landscape is the point of attraction for a new settlement. At each time step, which is designed to represent one year in the real-world scale, three consecutive phases take place: growth, aggregation, and allocation. In the first phase, a set of new agents is introduced to the model based on the population *growth rate* that is set as a parameter at the setup of the model. Each new agent chooses one of the closest empty cells to the center and establishes its singleton group. This location serves as its home-based location and affects the proximity calculation for mobility in the decision-making process. Initially, each agent only

occupies one unit of space, represented by a circle with surface area of one³. In the model landscape, each circle represents the footprint of a building containing a group.

In the next phase of the same time step, all of the agents in the model make a decision whether to move to a new group or to stay in their current group. Programming wise, they move sequentially, and thus the decision of each agent has an effect on all other agent's decisions in the time step (year). This mechanism is the closest representation of real-world decision-making process. However, I will test alternative event-sequencing mechanisms and their effect on the outcome pattern of the model in my future research. During each decision-making event, the active agent evaluates all of its possible choices based on their size and location. Each agent interacts with agents that are located within its *vision*. So, the possible destination choices are the groups to which the neighboring agents belong. The *vision*, is a parameter set exogenously at the beginning of each experiment, and defines the distance to which each agent can see and evaluate the environment. This variable along with the home-finding algorithm (in the growth process) are responsible for the influence of physical proximity in the evolution of the simulated city.

The size of each group is simply the number of members inside it. The chance of growth for each group depends on two factors: first, the number of members, which defines the size of that group; and second, the proximity of the group to other groups. These two endogenous factors, size and proximity, comprise the attraction forces in the aggregation process of the model. When an active agent wants to pick a new group to move to, among the groups of the agents that are inside the *vision-radius* of the agent, the larger groups have a better chance of being picked compared to

³A circle is selected as the shape representing building footprints for two reasons: First, a circle is the only uniform geometric shape that has constant distance from center to any point on the perimeter. Once a circle grows, the growth distributes uniformly in every direction. Second: the composition of circles with various sizes in a limited space can be programmed more easily than any other geometric shape. Two neighboring circles (as close to each other as possible but not overlapping) can only have one position that is being tangent. However, the composition is more complex for shapes that have multiple sides and edges.

smaller groups. Thus, in the first time step, when all the groups have only one member, all of the neighboring groups of an agent have the same chance of being picked and grow. In such case, the agent picks a group randomly.

In the general case, the probability of each group to be picked is directly proportional to its size. This part of the model is adopted from concept of Preferential Attachment (PA) or “the rich gets richer” process, in which a quantity is distributed among individuals based on how much they already have (Barabasi & Albert 1999). A combination of PA and growth, which are the two key ingredients of the real networks, is modeled by Barabasi and Albert (2002). They show that such systems generate scale-invariant properties in the network degree distribution. Their model implies that the more connected a node is, the more likely it is to receive new links. This general mechanism, with major changes forms the basis of the group formation process of my model. As such, the probability of any group to grow by a new member partly depends on how many members it already has.

If $A_{i,v}$ is the list of all the groups within radius $v = vision$ of the active agent i , then the probability ($P_{i,j}$) of group j from list A being picked by agent i is as follows:

$$A_{i,v} = \{group\ j : d_{i,j} \leq v\}, \quad (4-1)$$

$$P_{i,j} = \frac{S_j}{\sum_{k=0}^n S_k}$$

where, d_{ij} is the Euclidean distance between agent i and group j ; and S_j is the size of group j , which is equal to the number of members in this group. Although the distance between the active agent and the target group is not explicitly included in the equation above, it is inherited in the process, where the agent filters its choices based on distance. In fact, only the groups within certain distance can enter the competition to grow –the groups that are listed in *list A*. This list also includes the group in which the agent is already a member. So, in case the agent picks its owns group, it will

not move. If the agent is already a member of a large group, it is very likely that it stays in its current group and does not move.

It is important to note that the model is not deterministic, which means that agents do not compare their choices and simply select the largest one. Rather, the model is stochastic, implying that agents may pick any of the neighboring groups, but larger groups have a proportionally higher chance of being picked. This stochastic characteristic of the decision-making process ensures the representiveness of the model and encapsulates the random behavior in the real-world decision-making and aggregation process. It also matches with the well-known PA concept in small-world networks (Barabasi & Albert 1999).

The third phase, which is the building allocation phase, starts after all of the agents have made their moves. In this phase, buildings are updated based on the users' demands. For example, imagine a building contains a group with certain number of users. In the decision making phase, the group may have lost few members but received a lot more new members. Obviously, it requires more space to accommodate more group activities. So, the containing building needs to grow in size as well. In this phase, the building grows in place so that its new area equals to the number of members.

In real world growth process, generally, if the area is packed with neighboring buildings and there is not enough room to grow to the desired size, the building retains the floor area and grows in height in a way that the volume of the building approximately reflects the number of users. As the model landscape in Netlogo is represented in 2D, the volume cannot be represented explicitly. For the purpose of the present model, I exclude the three-dimensional representation of the built environment and assume that activities can only take place on the two-dimensional plane. This implies that larger buildings necessarily have larger footprints. Inevitably, the current process of representing buildings updates in the model may result in slight shifts in building centroids to allow

its growth. However, in future versions of the model I plan to apply density representations to prevent unrealistic dislocations. The summary of the code structure of the model in Netlogo is summarized in the pseudo code block in Figure (4-2). Also, Figure (4-3) illustrates model design and event sequencing in a flowchart diagram⁴.

```
Model variables:
  globals [initial-n-of-people, initial-city-extent, pop-growth-rate,
           newcomers, n-of-people, n-of-groups, city-extent, free-
           sites]
  agents-own [My-home, My-group, Vision]
  groups-own [members-list, n-of-members, area, d-center, ]

Model setup:
  To setup [
    setup-landscape []
    setup-agents [initial-n-of-people, initial-city-extent] []
    update-globals []
  ]

Each iteration:
  To go [
    grow [pop-growth-rate, n-of-people, free-sites] [
      introduce-newcomers []
      find-home []
    ]
    ask agents [
      find-new-group [my-home, vision] []
      sign-off-with-old-group []
      sign-in-with-new-group []
      move-to-new-group []
    ]
    update-groups [members-list, n-of-members] []
    update-landscape []
    update-globals []
    update-plots []
    output-results []
  ]
```

Figure (4-2): Main pseudo code block of the model.

⁴ The full code document of the model is accessible by request.

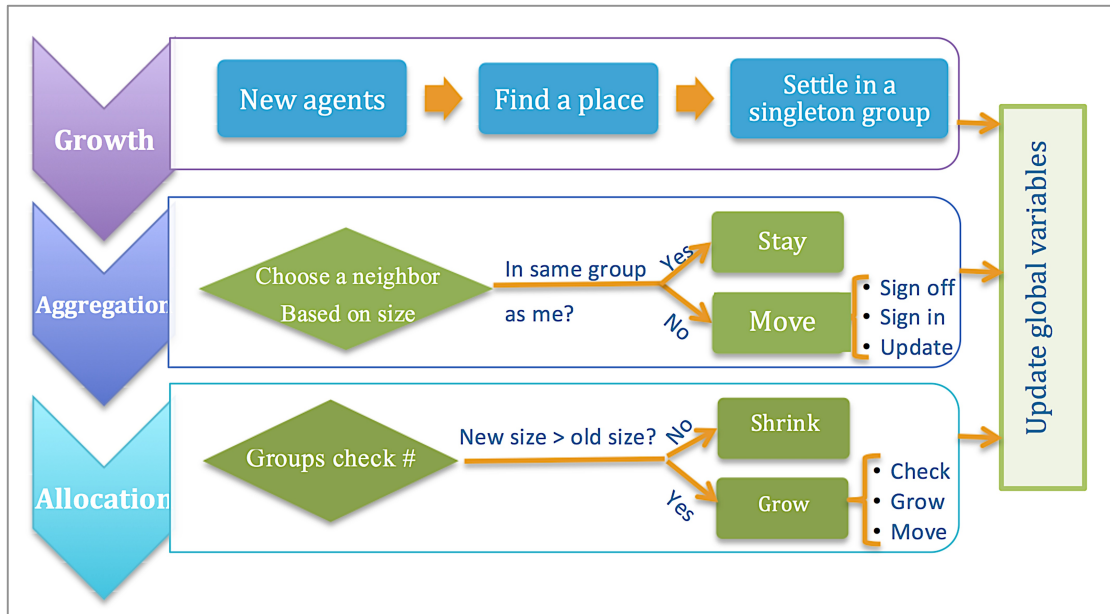


Figure (4-3): Flowchart summarizing model structure. The model consists of three main processes: growth, aggregation, and allocation that take place sequentially. In the growth process, new agents are introduced to the system based on the population growth parameter, and they find a place near other agents and settle down in a singleton group. In the aggregation process, each agent choose a group inside its vision radius based on the size of the groups such that larger groups have a better chance of being selected than smaller groups. The agent then check if the selected group is the same as its own group, if not, it will move to the new group. Finally, in the allocation process the model updates buildings sizes based on their new group size. For this purpose, groups check if the number of their member has been increased or not, then they will shrink or grow their building accordingly.

4.3.1 Model assumptions

As I am more interested in generating global patterns in my model rather than representing every real-world process specifically, I filter out unnecessary details (that are discussed later) as much as possible. I uphold to this strategy through out the whole model construction process in order to develop the simplest and most fundamental aggregation model of urban form. Once the basics are founded, building details can improve the representativeness of the model further.

I made several different generalized assumptions in this model. First of all, in real cities population clusters in many different ways, allowing for multiple memberships in various types of groups. However, in my model individuals can only be involved in one activity group at a time, which is meant to represent their most essential association; their employment.

The second generalized assumption in this model accounts for activity types. Although in real cities the density of population in each building depends on the land use and activity type, in the present model no distinction is made between different uses. I assume a standard space of one unit area is required for each agent regardless of location and density.

Third, although in the real world the population growth rate varies over time, I assume a constant growth rate throughout model iterations. This growth rate summarizes all reproduction, mortalities, and migration in a city. Finally, the same generalization is made for vision value, which is considered constant and discrete for every agent throughout the model. This parameter represents the extent to which the agent feels comfortable to travel from its home location and affects the number of choices that it considers in its decision-making process. In real-world scenario, vision value is different for every person, but for simplicity I assume that it stays constant for every agent during each model run. In the future extensions of this model, I plan to experiment with heterogenous preferences.

In the next chapter, simulation results and model landscapes are presented and analyses are discussed.

Chapter 5:

Results

This chapter is dedicated to the illustration of the simulation results and outcome landscapes from the model that was described in Chapter 4. At first, model parameters and settings are demonstrated. Then, a typical model landscape is established and analyzed for a fractal pattern. The model is verified and tested against a null hypothesis to show functional correctness. Finally, several experiments are performed to define the effect of model parameters on the landscape and resulting distributions. The chapter ends with an extensive discussion on the results and analysis.

5.1 Initial Settings, and Model Schedule

The model interface consists of a two-dimensional plain landscape, the exogenous parameters, rank-size distribution graphs, model monitors, and outputs, as demonstrated in Figure (5-1) below. The initial parameters include: *initial number of people*, *initial extent of the city*, *population growth rate*, *vision*, *population limit*, and *number of simulation runs*. The initial number of people and initial city extent define the setup of the landscape and are set to 50 people in a 14-unit radius from the center of the landscape as a default. The base case setup of the landscape is demonstrated in Figure (5-1); white buildings are randomly allocated in green landscape. When the “go” button is hit, new people are introduced to the city based on the population growth rate and look for free sites near the city center. Then all the agents start to interact with their neighbors in their vision radius and join them to make a group. The model is set to stop when the population reaches 20,000 agents, for consistency of the results and validity of comparisons.

| Model Attribute | Range | Base case value |
|--------------------------|------------|--|
| Initial number of people | 1-100 | 50 |
| Population limit | 20,000 | The model stops when the population reaches 20,000 |
| Population growth rate | 0.01 – 0.1 | 0.08 |
| Initial city extent | 1-20 | 14 |
| Vision | 0-100 | 5 |
| Agent activation | Random | Random |
| Initial condition | - | All agents in singleton groups |

Table (5-1): Model parameter range and 'base case' values

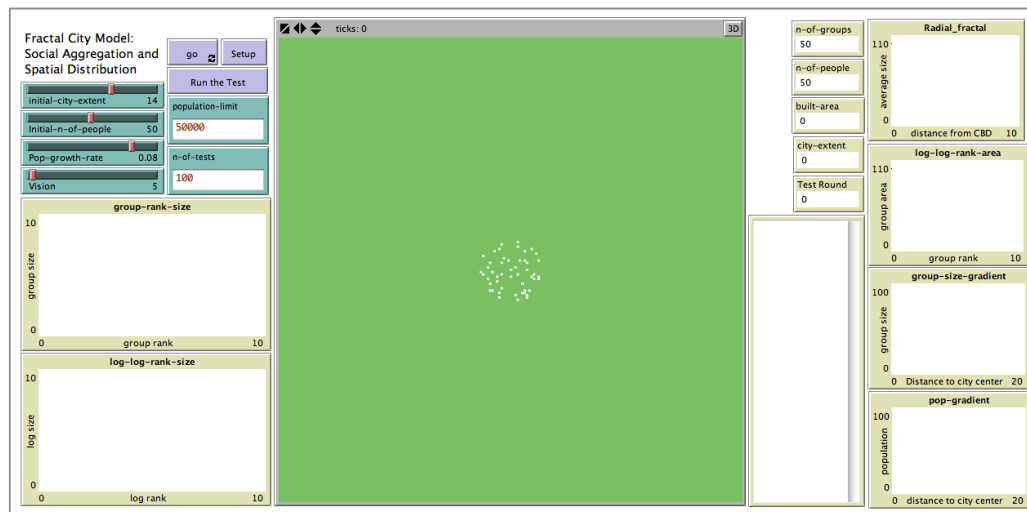


Figure (5-1) : Model interface in Netlogo® consisting of 2D landscape, model parameters, distribution graphs and monitors.

The scheduling of the model is designed to approximate the real world aggregation process. In this way, agents take action one by one, so that the decision of each agent affects the decision of the next agents. By the end of each iteration, all the agents including the new ones, which have been born or immigrated to the system, and the old ones from last iterations have made a decision whether to stay in their group, or to join other groups. Then, all the monitors and graphs are updated to reflect the instant changes in the model variables as the time proceeds.

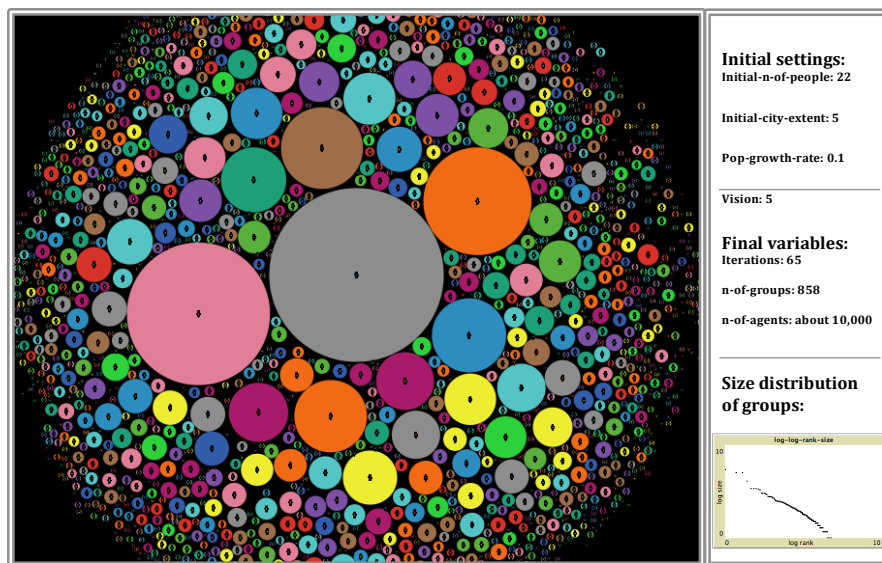


Figure (5-2): Model outcome landscape in Netlogo®. Each circle represents a building housing an activity group with single floor height. Colors are random, but sizes are proportional to the size of the group using the building. The window size is only visual and does not show the actual landscape boundaries.

5.2 Model landscape and result analysis:

In almost all the model landscapes, a similar overall pattern emerges. In this section I demonstrate the outcome landscape of a typical model and provide a fractal analysis exploring the research hypothesis. Typically, the model generates power law distributed buildings in the landscape with decreasing building sizes from city center. Figure (5-2) shows the outcome landscape of the model with the given initial parameters in Netlogo®. The landscape size is set to be large enough in order not to impose any boundary effect on the landscape pattern. Each circle in the model

represents a building with a certain size that is proportional to the size of the group using it. Once the point location of buildings and their size is defined in Netlogo®, the data is then transferred to Repast® for parcel subdivisions. With the GIS capabilities of Repast®, parcel representations are generated in a Voronoi display. Figure (5-3) displays the parcel subdivisions in the model landscape based on the Weighted Voronoi Algorithm described earlier. Building locations serve as the polygon centroids and buildings sizes are transferred as weight in the Voronoi diagram.

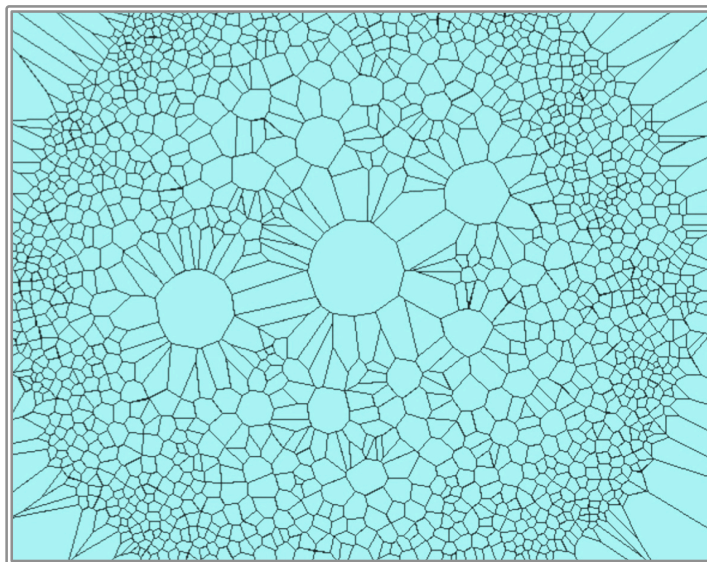


Figure (5-3): Voronoi Illustration of Parcel Distribution in Simulated City (created in Repast®). Each polygon in the landscape represents a parcel in the simulated city with an area that is proportional to the number of individuals using the land.

Before I move on to analysis, it is important to note that the intention of this section is not to look at whether the distribution of groups are consistent with that of buildings, but rather the goal is to examine the conformity of the outcome landscape to the real-world patterns. As discussed in Chapter 4, the model is designed to reflect the hypothesized process and to examine both statistical and spatial patterns of the outcome landscape.

My first foray into analysis looks at scaling in the size distribution of buildings. Figure (5-4) indicates the log-log graph of the rank-size distribution of buildings generated by the model. There is very clear scaling in the data with a coefficient of determination (R^2) of 0.975 to the power law

model. Table (5-1) summarizes the parameters of the regression analysis. The slope of the power law model fitted to the buildings area is 0.769, which is very close to the slope of 0.763 of the area-distribution of buildings from all land-uses in London, UK (Batty et al., 2007).

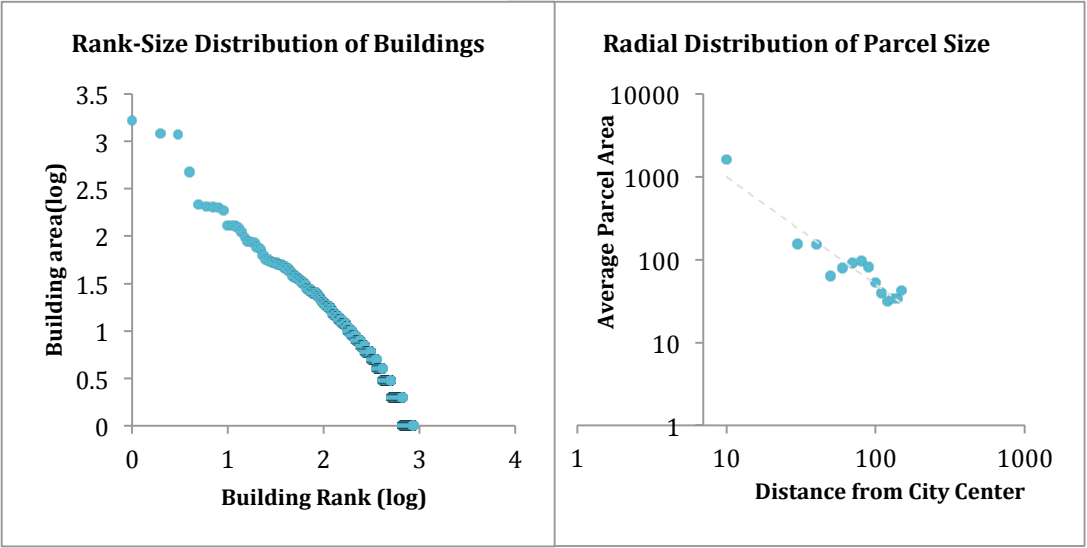


Figure (5-4): Left: rank-Size distribution of buildings by area on a log-log plot revealing power-law. Right: radial distribution of parcels by area.

| | <i>Coefficients</i> | <i>Standard Error</i> | <i>t Stat</i> | <i>P-value</i> |
|------------------|---------------------|-----------------------|---------------|----------------|
| Intercept | 2.975 | 0.004 | 640.121 | 0.00 |
| Power | -0.769 | 0.005 | -135.915 | 0.00 |

Table (5-2): Power law parameters of regression analysis for buildings area

Secondly, I look at the spatial distribution of buildings based on their distance from the center. In Figure (5-4), the radial distribution analysis of parcels from Figure (5-3) is presented. In this graph, the parcels are classified according to their distance from the center. Then the average area of each class is plotted on the Y-axis. I show quite conclusively that the distribution can be approximated by rank-size distributions that imply power laws. However, it is important to note that the adjustment of the radial distribution to the power law model is less strong compared to the rank-size graph as can be concluded from the R-squared of only 0.90. This is due to two sets of problems: first, as the simulated city is two-dimensional, the buildings grow on the surface with uniform

density, and thus the huge area covered by the few central parcels made the graph unconnected; and second, the number of observations, which is the distance intervals from city center, is limited.

The overall pattern of the radial distribution graph agrees with the general observation in cities, where the concentration of large institutions and businesses takes place near CBD (Clapp 1980; Erickson and Wasylenko 1981; Lee 1982; Ihlanfeldt and Raper 1990; Shukla and Waddell 1991; Coffey et al. 1996; Yarish 1998; Wu 1999). There is, however, a major difference between this model and the land subdivision process in urban growth. In real-world cities, people compete for the lands near the CBD. Once all the land is occupied, further development take place in the form of further subdivision of the existing parcels and land-intensification in the third dimension. So, the buildings in the CBD do not necessarily have larger areas; but rather have larger volumes (e.g. building area times building height). Activities that require large building footprints (such as most industrial uses) move to suburbs with larger available parcels. In my model, these two processes (that is relocation and intensification processes) are excluded. The building footprints and parcel areas in the model landscape represents the building volumes. As demonstrated in Figure (5-3), as the distance to the center increases, the size of the parcel decreases. The radial-distribution graph in Figure (5-4) shows that this decline follows a power-law structure. The combination of results from the rank-size distribution analysis and the radial-distribution analysis confirms that the simulated landscape as a whole, exhibits fractal-distributed buildings.

5.3 Model verification

Model verification refers to ensuring that the model performs the way it is designed for. In this section the processes that are used to verify the model are discussed. First, the code structure and results are checked for the following functions through the variable monitors in the model interface:

- Each agent can only be in one building at any time, so that the sum of building users

are equal to the agent population at any time.

- Building footprints are proportional to the number of users
- No overlapping is allowed for buildings in the landscape, so the total building footprint is equal to the number of agents in the model.

Secondly, verification of the model is made by repeatedly running the model for the same set of parameters for 100 times, and monitoring the precision of results. Figure (5-5) and (5-6) shows the result of the regression analysis for all of the tests. The first graph confirms that the slope of the fitted line for the power-law model stays stable around the value of $D = 1.27$. The second graph (Figure (5-6)) presents the R-squared values for D values achieved for each test. R-squares are also stable throughout the 100 runs and show an average of $R^2 = 0.97$.

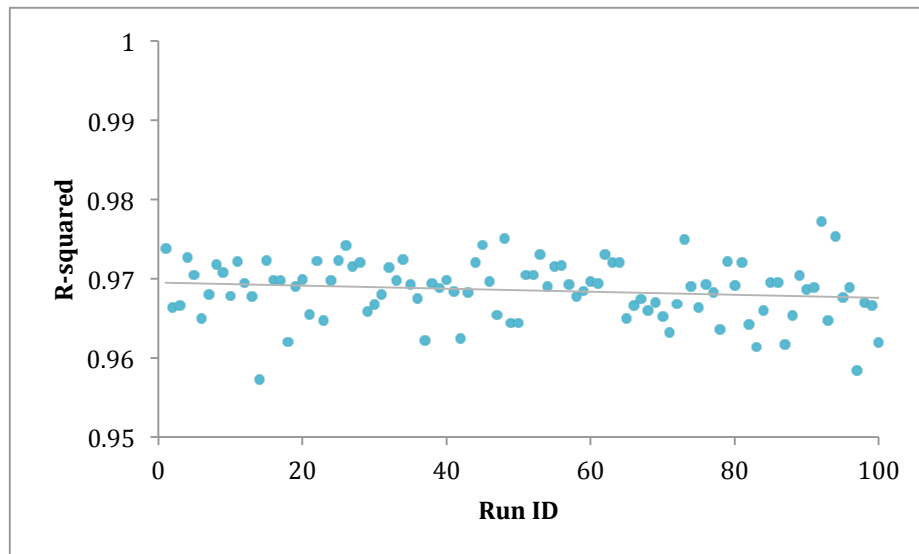


Figure (5-5): Distribution of R-squared for the power law model fitted to the verification tests (100 runs of the model with same parameter values), showing high and stable r-squared for all the tests.

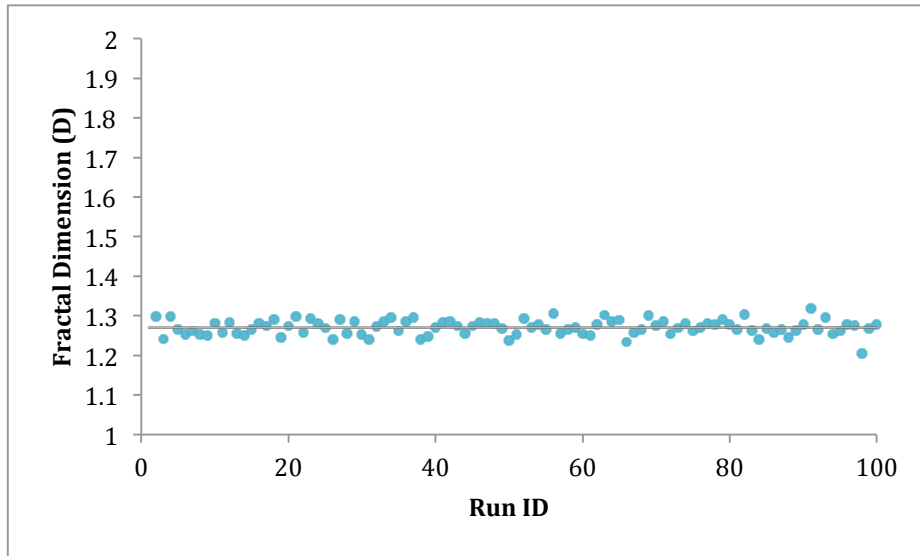


Figure (5-6): Distribution of fractal dimension of verification tests (100 run with same parameter values), showing stable values around $D=1.27$ for all the tests.

5.3.1 Null Hypothesis

In order to verify that the power law pattern that is observed in the simulation landscape is not a result of random distribution of variables or artifact of spatial distribution of agents, a null scenario is designed and tested. Unlike the model decision-making process, where the probability of each neighbor groups, being selected by an agent was proportional to its size, in this scenario, the aggregation process is based on the random selection of neighbor groups. All other functions and parameters in the model remain the same. Figure (5-7) demonstrates the outcome landscape of the null model. The radial and rank-size distributions of the buildings are represented in Figure (5-8) and (5-9) respectively. It is clear that there is no significant correlation between the distance from the city center and the size of buildings. Also, the variation of building sizes is considerably limited compared to the initial model where the distribution followed a power law pattern with few very large buildings; some mid-size buildings and the majority were small size units.

The result shows that the missing mechanisms were responsible for the aggregation of the population into larger groups and creating a large variation of group sizes in the city. The results highlight the importance of size in the aggregation process in cities, which means that people not only like to make groups with each other to live and work more efficiently, but also, they prefer to be in larger groups and activities. Furthermore, the preferential attachment mechanism is responsible for the radial distribution of buildings where the concentration of population takes place near CBD. The primary theories of urban evolution (Clark 1951; Stewart & Warntz 1958; Batty & Kim 1992) recognize the transportation cost as the key reason why the population density declines with the

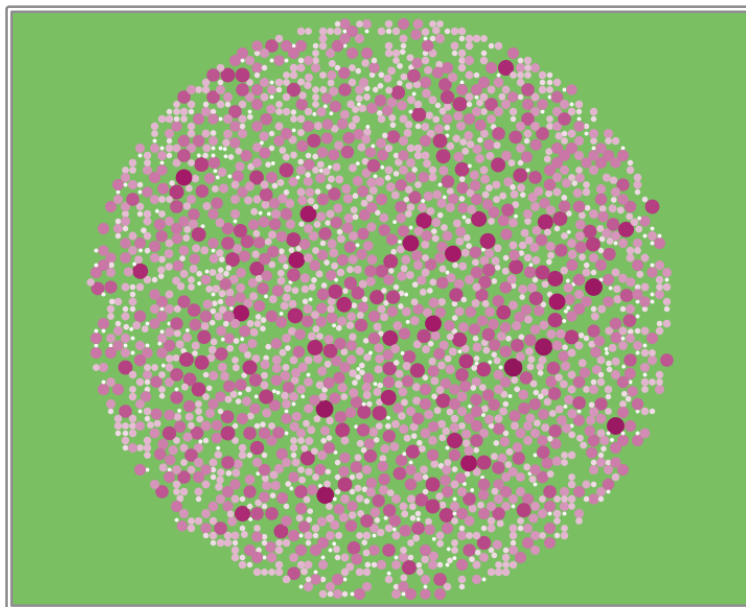


Figure (5-7): Simulated landscape from null hypothesis revealing dispersed size distribution. Each circle represents a building in containing a group. They are color-coded by the number of users so that, the darker the color, the larger the number of users of that building.

distance from the city center. The result of this study complements the above theory by explaining that the attraction to CBD is the result of the existence of larger activity groups (including institutions, businesses, and leisure) and better opportunities in the center; simply because the groups in the center have been around and developed for longer period of time. As demonstrated in the null model, the transportation cost by itself (represented by *vision-radius* in the model), creates a circular city shape (which is the most efficient shape in regard to distance to a point), but does not generate a density gradient. Further elaboration of this argument is discussed in Section 5.5.

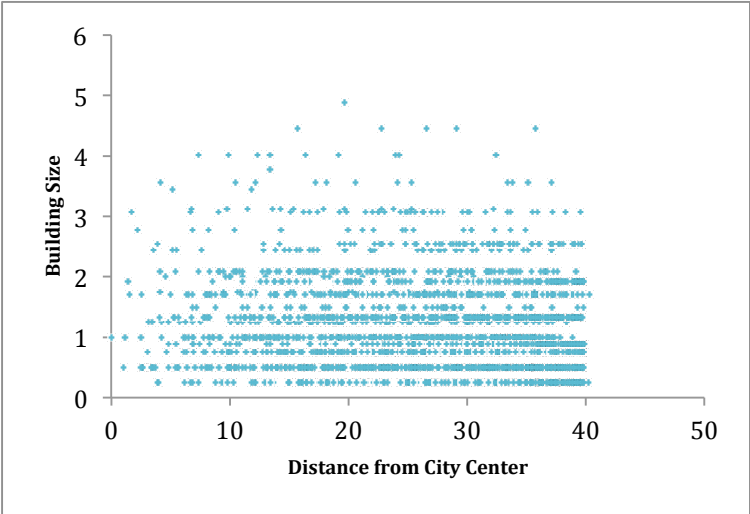


Figure (5-8): Radial Distribution of buildings in the null hypothesis

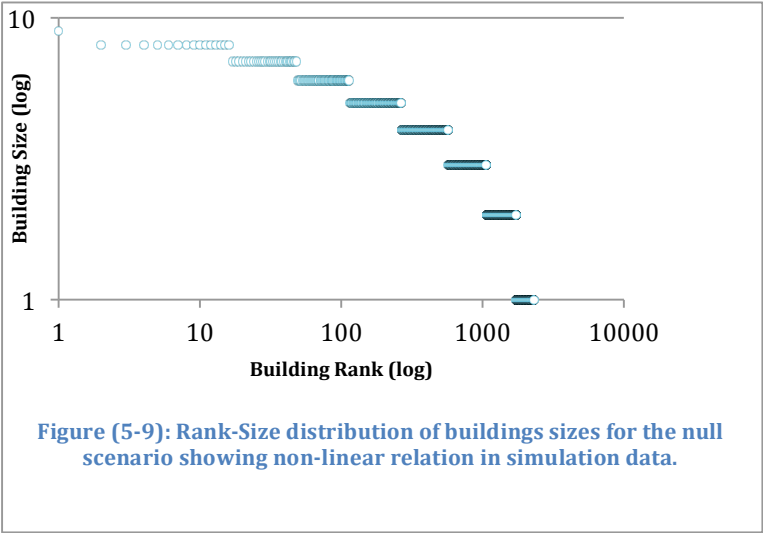


Figure (5-9): Rank-Size distribution of buildings sizes for the null scenario showing non-linear relation in simulation data.

5.4 Experiments

5.4.1 Effect of Population Growth Rate on the Model Landscape

An important component of the model mechanism is the growth dynamic, which implies that the number of agents in the model starts from a limited number defined at the setting and continues to grow by a defined growth rate as the model iterates. The dynamic property of the model is one of the key factors responsible for the emerging fractal pattern in the system. In this section I explore the effect of the population growth rate on the fractal dimension of the

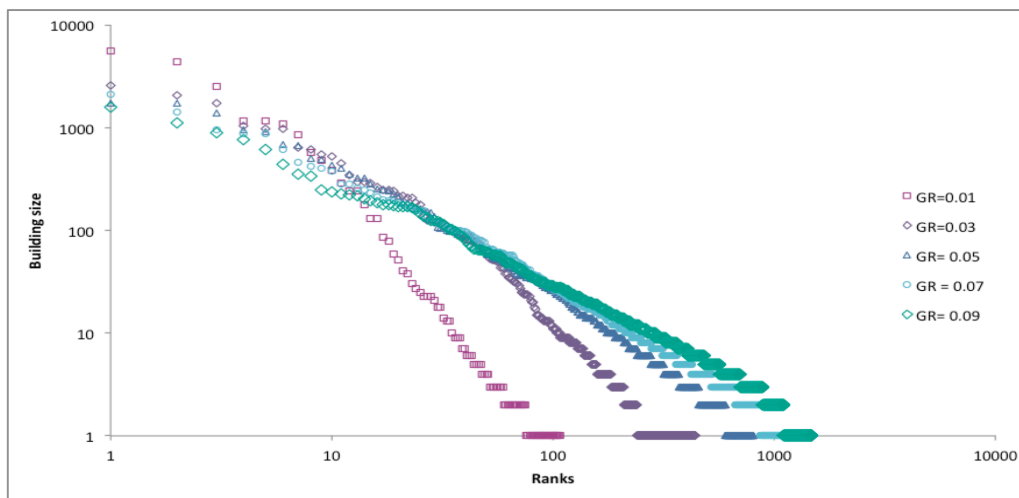


Figure (5-10): Rank-size distribution of buildings' size from the tests of different Population Growth Rates (GR) distribution of the buildings in the simulated landscapes. For this purpose, experiments with 10 variation of the growth rate ($0.01 < \text{growth rate (GR)} < 0.1$) have been conducted. For clarity and organization purposes, the results of only five of them are presented here in Figure (5-10).

Visual evaluation of the graphs shows that the distributions can be regarded as two parts: upper graphs consisting of approximately the largest 10 buildings, and lower graph made up of the majority of the buildings, which are smaller. The upper graphs of the experiments are more similar to each other compared to the lower parts, which suggest that the effect of population growth rate is mostly seen toward the tails of the graphs. This can be explained by the definition of the preferential

attachment equation (4-1). The growth of the population by each person increases both the nominator and the denominator of the equation. However, the increase in the value of the denominator is larger than the nominator. That means the attraction force of smaller groups drops more significantly by growth of the population compared to larger groups. As a result, there is more separation between the tails than the heads. This also explains why, among the first-rank buildings, the largest one belongs to the model with the lowest growth rate, and the smallest belongs to the model with the largest growth rate. A higher growth rate implies that in each iteration, the number of newcomers (and thus startup groups) to compete with large groups is larger. So, the large group will have less chance of growth resulting in lower maximum size in the whole system.

Table (5-3) summarizes the experiment analysis for the variation of population growth rates. It shows that the fractal dimension (D) decreases with an increase in the growth rate. As discussed above, this behavior is due to the less competition brought about by the low growth rate, which increases the scaling power of size effect. Also, the results indicate that the extent (maximum radius) of the simulated city increases significantly with an increase in the growth rate. This increase is consistent with the increase in the number of buildings. It can be explained by the fact that a lower growth rate increases the chance for the population to aggregate in the older and larger groups, so the total number of groups will decrease. In general, this experiment shows that population growth works as a disaggregating force in the evolution of a city, which is highly consistent with real-world stylized result (e.g. study of urban spatial structure by Anas et al. (1998))

Table (5-3): Experiment results for variation of population growth rate.

| Growth rate | Number of buildings/groups | Max building size | City extent | D | R ² |
|-------------|----------------------------|-------------------|-------------|------|----------------|
| 0.01 | 107 | 5522 | 10.05 | 2.38 | 0.97 |
| 0.03 | 440 | 2553 | 16.56 | 1.81 | 0.96 |
| 0.05 | 806 | 1742 | 25 | 1.46 | 0.98 |
| 0.07 | 1189 | 2117 | 29.27 | 1.32 | 0.98 |
| 0.09 | 1479 | 1572 | 32.76 | 1.22 | 0.96 |

5.4.2 Effect of Vision-Radius on the Model Landscape

Vision is an exogenous parameter that plays an important role in the model. It works as the neighborhood effect in most CA models, and defines the extent to which each agent can see, evaluate and move in its environment. *Vision* is designed to summarize two factors: first, the size of the agent's primary network (dependent on spatial proximity), second, the distance in which the agent can move (which is dependent of the transportation cost). In this section I explore the effect of the *vision* value on the spatial distribution on the buildings in the simulated landscapes. For this purpose, experiments have been run with four variation of the parameter (ranging from minimum of 10 and maximum of 70). The rank-size distribution of buildings for all experiment landscape is presented here in Figure (5-11).

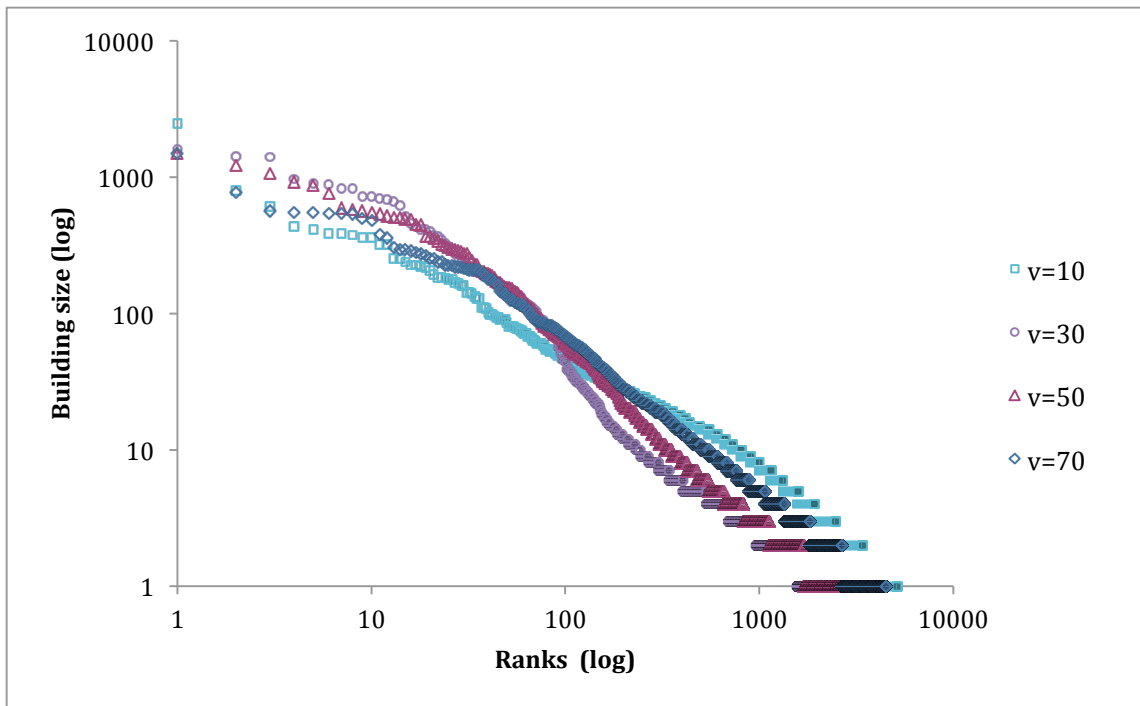


Figure (5-11): Rank-size distribution of buildings in the experiment landscapes.

The visual representation of the graphs show very similar behavior in all four experiments, following a straight line specially in the middle and low ranks. Summaries of the model statistics are

provided in Table (5-4). The total population is similar for all experiments, as they have a growth rate of 0.1 and have iterated for 60 time steps. Experiment one, with vision-radius of $v = 10$, has the largest number of formed groups at the end of the simulation. This is due to the fact that it takes a longer time for new agents with shorter vision to aggregate. As most of new agents arrive at the periphery of the city, they require more steps to reach to larger groups that are mainly located in the CBD. So, in a given time, short-vision agents can travel shorter distances toward city center and can aggregate into smaller groups on average. This results in the larger overall number of groups in the landscape.

| Experiment | Vision | Number of buildings/groups | Maximum building size | D | R ² |
|------------|--------|----------------------------|-----------------------|------|----------------|
| 1 | 10 | 5101 | 2462 | 1.09 | 0.95 |
| 2 | 30 | 2994 | 1617 | 1.13 | 0.96 |
| 3 | 50 | 3203 | 1493 | 1.2 | 0.98 |
| 4 | 70 | 4498 | 1496 | 1.13 | 0.98 |

Table (5-4): Fractal dimension of simulated landscapes for vision experiments

The rank-size fractal dimension (D) is calculated for each landscape with very high R-squared values as demonstrated in the table. The results show that the value of D increases with the increase in agent's vision-radius. This effect can be due to the fact that an increase in vision value leads to a larger network and more interactions in each decision-making event. It increases the competition and chance of growth for a higher number of groups, which leads to larger power coefficient (slope) in the power-law model.

According to Table (5-3), experiment 4, which has the largest vision value ($v = 70$), disobeys the trend of increased fractal dimension with increasing vision. In order to explain this behavior, the relationship between the values of vision-radius and the radius of the simulated city is outlined in Figure (5-12). In all of the experiments, the maximum radius of the simulated city at its largest state ($t = 60$) is approximately 70 units, which equals to the vision-radius of experiment 4. The diagram shows one of the most remote agents in the city, who lives in the periphery with 70-unit distance to CBD. This agent represents newcomers in the city who occupy the smallest groups. Increasing vision-radius of the displayed agent, from experiment 1 to 4, increases the access domain of the agent to the larger number of groups. Exceptionally, experiment 4, is the only scenario that provides a domain for the newcomers that includes CBD, where the largest groups are located. In this scenario, on one hand, every agent in the city has access to CBD and on the other hand, they are reachable by central groups. This creates a more distributed pattern and thus, a slight decrease in the fractal dimension of the size-distribution in the landscape.

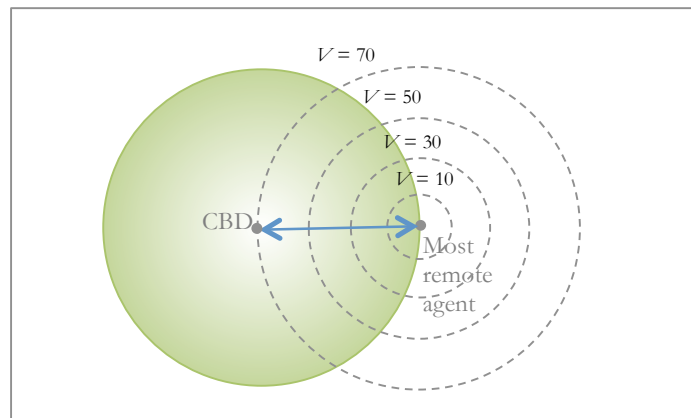


Figure (5-12): Diagram showing the experiment vision value in reference to CBD.

5.5 Discussion

In this chapter, the outcome patterns of the model landscapes were presented and discussed. The model is intended to represent the aggregation process in the evolution of urban form in the most abstract way. So, the validation of the model relies on the overall conformity of the size and radial distribution patterns of the simulated landscapes to those generally observed in the real cities. In chapter 2, I discussed that a power law can approximate the size distribution of buildings in most cities. Thus, I use a qualitative validation of the model outcome to patterns of urban form. Also, the effects of the model variables such as population growth rate and vision-radius on the landscape patterns are tested. The results show that increasing vision-radius has a positive effect on the value of the fractal dimension, while the growth rate of the population has a negative effect. These are the underlying forces that explain the fractal pattern in the system. The attraction to larger groups inside the vision-radius works as an aggregating force, and the space constraint and population growth play the segregating forces. The balance between these forces defines the slope of the power-law model and consequently, the fractal dimension of the system.

The preferential attachment mechanism that is built in the model is different from that of Barabasi-Albert (BA) model in two main ways. First, in the BA model agents do not join together, but rather, they create links to other nodes in the systems. So, even after they connect to someone, they continue to exist as an independent node and can be selected by new agents to create links with. However, in my model once an agent joins a group, it leaves its previous group and place. Second, in the BA model, agents can make a decision only once in their lifetime, and once the decision is made, it cannot change; but, in my model, the agents make decision in each time step and update their status based on their previous status and the new environment. As power law patterns emerge in the aggregate distribution of the buildings in the simulated landscape, we can conclude that the fractality of the model is generated primarily from the recursion of the competition process between

aggregating and segregating forces. All other mechanism and details (such as frequency of decision-making, spatial layout algorithm, and group to building allocation process) are secondary.

One of the key findings of this research is to confirm that “history” plays an important role in modeling the urban growth dynamic. When the model starts with few agents representing the first settlers in a city and then grow to a desired population, the City Center and the development pattern emerge as the effect of the time and the place that has the longest history of interaction. In other words, the location of City Center or CBD is path-dependent and does not have an independent meaning without the history of the city. As we can see in the model, the transportation cost as the distance to CBD is not explicitly modeled. However, the model forms a circular pattern similar to that of urban growth models with an inherent function of transportation cost to CBD. This is due to the fact that attraction to CBD is a result of long history of the location of CBD in hosting most of the interactions and activities. Thus, modeling the attraction to larger groups and activities in the city has successfully replaced the traditional method of modeling transportation cost to CBD explicitly.

As the model is designed to be very abstract, it includes only the fundamental mechanisms that are proposed to be involved in generating fractal patterns in urban landscapes. Therefore, the model excludes many real-world mechanisms associated with the growth process. For example, multiple membership processes are simplified into single memberships that represent the employment association of each person. Also, agents are assumed to be homogeneous in their preferences of group size, proximity, and frequency of decision-making. Another major simplification that is made in this model is in the building allocation process as listed below:

- Groups occupy buildings that are necessarily proportional to their size (number of members).
- No more than one group can use one building.
- Buildings have uniform density and can only expand on the 2D plane.

- Moving of a group as a whole to a new location is not modeled.

In order to better represent the real-world urban growth processes, the future extension of this model need to include the above components.

6.1 Study Overview

Despite all the advancements in the urban science, we still lack a comprehensive understanding of how cities work and how various facets of cities are intertwined. In this thesis I have narrowed down the scope of this question and looked at the similar patterns in the social and spatial properties of cities. Several studies indicate that the urban form patterns reveal fractal properties both in the size-distribution of buildings, parcels and roads and also in the spatial configuration (White and Engelen 1993; Batty & Longley 1994; Frankhauser 1994). Also, numerous studies in the social science suggest that the aggregate distribution of groups, firms, and organizations follow a power-law pattern, which is a key characteristic of fractal systems (Axtell 2001; Zhou et al. 2005; H. Aoyama et al. 2009). According to the similarities in these observations, I have hypothesized that the fractal pattern in the urban form emerges as a result of human aggregation into activity groups over time. As buildings are the containers of human activity, the same overall distribution as in group sizes emerges in building distribution, with some spatial and temporal alterations.

As a starting point in the examination of the proposed hypothesis, I adopted a process-based theoretical approach of computer simulation. A computational laboratory provides a virtual environment that enables researchers to explore the validity of certain abstract hypothesis theoretically. In particular, for processes that take place over a long period of time, where empirical exceeds the standard capacity and scope of individual endeavor, computer simulation are of particular interest. In the case of my hypothesis, since it suggests a new description for the evolution of urban form from human aggregation process, empirical methodologies fall short to fully examine

it. For this purpose, I have developed a very abstract agent-based model of a typical town that consists of homogeneous agents in a featureless landscape. As the model iterates, the population of agents grows and agents start to interact with each other and aggregate into groups of various sizes. The groups then start to settle into buildings that are proportional to the number of users in each. The simulation results were used to analyze whether the proposed hypothesis generates building distributions that are similar to those of real-world urban landscapes.

Verification and validation tests were performed using a null hypothesis and fractal analysis respectively. The results strongly revealed fractal patterns in the size-distribution of buildings in the landscape, with a fractal dimension very close to that of London, UK's buildings as calculated by Batty et al. (2007). The landscape also exhibits a radial distribution of building sizes that decreases exponentially with distance from city center. This behavior resembles the exponential decline of population density in real-world urban areas (Clark 1951, Batty 2007). Experimenting with the effects of model parameters, it is inferred quite conclusively that fractal dimension increases with increasing vision-radius and decreasing population growth rate. Also, the model strongly suggests that including two components of history and vision-radius in urban growth process can convincingly replace traditional transportation cost models to city center. In fact, the emerging radial pattern of the size-distribution of buildings, with larger sizes in the center and smaller size in the periphery, is the result of path dependent history of the model from interactions of agents near city center and their tendency to locate near already developed areas.

6.2 Future Direction

As the model is designed to be very abstract, to be able to show the result of the proposed hypothesis in isolation, several real-world processes that contribute in the evolution of urban form are excluded. These processes include: three-dimensional density, planning interventions (in both large and small scale), intra-urban network connectivity and employment mobility, group break

down and convergence, agent diversity of preferences, and multiple factors in the group formation process. The future expansion of this research needs to examine the aggregate effect of the excluded factors on the overall pattern of the simulated landscape. However, it is important to note that any computer models of urban dynamics are subject to abstraction and exclusion of some unknown factors. Thus, it is recommended that future studies support the model by conducting an empirical examination of the correlation between the aggregate pattern of group size distributions and the building size distributions in cities. This will shed light on the usefulness and accuracy of the model proposed in this research.

Currently, I am working on improving the model to include density and display the model output in three-dimensional space to better represent the radial density gradient in cities. Also, for my PhD program, I have proposed to establish the fractal approach as a new method in urban studies to infer the quantity and structure of socio-economic interactions by reading patterns of buildings datasets. In particular, I am aiming to study the interactions that lead to agglomeration of individuals in space in forms of socio-economic activities, which in turn influence the individual location choices. I intend to use fractal dimension as a measurement to compare the distribution of social and spatial structures in cities. I hypothesize that the size distribution of groups, firms and institutions in the city indicates the rate and scope of human interactions that have led to the formation of groups. My approach to find the correspondence between social and spatial structures is to compare the distribution of buildings to the distribution of socio-economic groups. The originality of this approach can pave the way for future studies to use complex measurements to infer socio-economic profile of cities from spatial patterns.

6.3 Planning and Policy Implications

The development of this research project leads to the establishment of a novel theory that unifies the divergent views on the evolution of cities in different disciplines to one that centers on

the interconnectedness of people in cities. The theory provides further support to the writings of pioneer advocates of planning for people such as Patrick Geddes (1949) and Jane Jacobs (1961), who value people as the main player in urban dynamics and believe that any planning interventions should be a response to the needs of citizens. This theory adds to their notion that, the different physical structures in urban form can be the reflection of different social structures. More specifically, the aggregation and segregation forces in social agglomeration process play significant roles in the formation of the built environment. The findings of this research encourage urban planners to identify the social side of aggregation and segregation forces to better plan for long-term changes in the built environment. For instance, in order to achieve higher fractal dimension in the landscape, which is correlated with intensification, planning and policy can harness the aggregation forces in urban dynamics including socio-economic collaboration, social capital and human connectivity, and employment mobility. This method will also assist to designing policies that encourage involvement of people in local groups and activities and improve ties to physical places in the city. It also supports designing mixed uses and variety of sizes to facilitate interaction of activities and formation of socio-economic groups. Using this bottom-up approach helps urban planning to achieve intensified landscapes in the long run.

By recognizing the linkages between socio-economic structures and their effect on urban form, the results of this study will further accelerate the development of simulation models that aim at projecting urban phenomena (Batty, 2005; Benenson and Torrens, 2004; Huang et al., 2014). It will also help planners to project urban growth distributions with more accuracy and confidence.

Bibliography

- Anas, A., Arnott, R., & Small, K. A. (1998). Urban spatial structure. *Journal of economic literature*, 1426-1464.
- Annenberg Foundation (2014). Fractal by nature, How long is the coastline of Britain? Annenberg Foundation website. <http://www.learner.org/courses/mathilluminated/units/5/textbook/07.php>
- Axelrod, R. M. (2006). *The evolution of cooperation*. Basic books.
- Batty, M. (1991). Cities as fractals: simulating growth and form. In *Fractals and chaos* (pp. 43-69). Springer New York.
- Batty, M., & Kim, K. S. (1992). Form follows function: reformulating urban population density functions. *Urban studies*, 29(7), 1043-1069.
- Batty, M., & Longley, P. A. (1994). *Fractal cities: a geometry of form and function*. Academic Press.
- Batty, M. (2007). *Cities and complexity: understanding cities with cellular automata, agent-based models, and fractals*. The MIT press.
- Batty, M. (2008). The size, scale, and shape of cities. *science*, 319(5864), 769-771.
- Bettencourt, L. M. (2013). The origins of scaling in cities. *science*, 340(6139), 1438-1441.
- Bourke, P. (2003). *Fractal Dimension Calculator user manual*. Swinburne University of Technology Web.
- Brown, D. G., Page, S., Riolo, R., Zellner, M., & Rand, W. (2005). Path dependence and the validation of agent-based spatial models of land use. *International Journal of Geographical Information Science*, 19(2), 153-174.
- Cooper, J., Watkinson, D., & Oskrochi, R. (2010). Fractal analysis and perception of visual quality in everyday street vistas. *Environment and planning. B, Planning & design*, 37(5), 808.
- Cooper, J., Su, M. L., & Oskrochi, R. (2013). The influence of fractal dimension and vegetation on the perceptions of streetscape quality in Taipei: with comparative comments made in

- relation to two British case studies. *Environment and Planning B: Planning and Design*, 40(1), 43-62.
- Chen, Y. (2012). Fractal dimension evolution and spatial replacement dynamics of urban growth. *Chaos, Solitons & Fractals*, 45(2), 115-124.
- Chen, Y. (2013a). Fractal analytical approach of urban form based on spatial correlation function. *Chaos, Solitons & Fractals*, 49, 47-60.
- Chen, Y. (2013b). A set of formulae on fractal dimension relations and its application to urban form. *Chaos, Solitons & Fractals*, 54, 150-158.
- Chen, Y., Li, X., Liu, X., & Ai, B. (2014). Modeling urban land-use dynamics in a fast developing city using the modified logistic cellular automaton with a patch-based simulation strategy. *International Journal of Geographical Information Science*, 28(2), 234-255.
- Clark, C. (1951). Urban population densities. *Journal of the Royal Statistical Society. Series A (General)*, 114(4), 490-496.
- Clapp J (1980) The intrametropolitan location of office activities, *Journal of Regional Science*, 20 (3), pp. 387-399
- Coffey W, Drolet R and Polese M (1996) The intrametropolitan location of high order services: patterns, factors and mobility in Montreal, *Papers in Regional Science*, 75 (3), pp. 293-323
- Cordoba, J. C. (2008) On the distribution of city sizes. *Journal of Urban Economics* 63, 177-197.
- Dauphiné, A. (2013). *Fractal Geography*. John Wiley & Sons.
- Erickson R and Wasylenko M (1980) Firm relocation and site selection in suburban municipalities, *Journal of Urban Economics*, 8, pp. 69-85
- Farmer, J. D., & Foley, D. (2009). The economy needs agent-based modelling. *Nature*, 460(7256), 685-686.
- Falconer, K. (2013). *Fractal geometry: mathematical foundations and applications*. John Wiley & Sons.
- Gabaix X, 1999, "Zipf's law for cities: an explanation" *The Quarterly Journal of Economics* 114, 739-767.

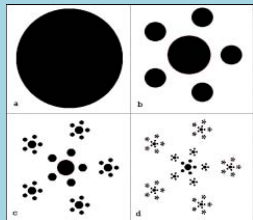
- Gil, J., Beirão, J. N., Montenegro, N., & Duarte, J. P. (2012). On the discovery of urban typologies: data mining the many dimensions of urban form. *Urban Morphology*, 16(1), 27.
- Goldberger, A. L., Amaral, L. A., Hausdorff, J. M., Ivanov, P. C., Peng, C. K., & Stanley, H. E. (2002). Fractal dynamics in physiology: alterations with disease and aging. *Proceedings of the National Academy of Sciences*, 99(suppl 1), 2466-2472.
- Ihlanfeldt K and Raper M (1990) The intrametropolitan location of new office firms, *Land Economics*, 66 (2), pp. 182-198
- Keersmaecker, M. L., Frankhauser, P., & Thomas, I. (2003). Using Fractal Dimensions for Characterizing Intra-urban Diversity: The Example of Brussels. *Geographical analysis*, 35(4), 310-328.
- Lee K (1982) A model of intraurban employment location: an application to Bogota, Colombia, *Journal of Urban Economics*, 12, pp. 263-279
- Mandelbrot, B. B. (1975). Stochastic models for the Earth's relief, the shape and the fractal dimension of the coastlines, and the number-area rule for islands. *Proceedings of the National Academy of Sciences*, 72(10), 3825-3828.
- Mandelbrot, B. (1990). *Fractals: a geometry of nature: fractal geometry is the key to understanding chaos. It is also the geometry of mountains, clouds and galaxies.* New Scientist, 127(1734), 38-43.
- Morgan, F., & O'Sullivan, D. (2009). Using binary space partitioning to generate urban spatial patterns. In 4th International Conference on Computers in Urban Planning and Urban Management, University of Hong Kong, Hong Kong.
- North, M.J., N.T. Collier, J. Ozik, E. Tatara, M. Altaweel, C.M. Macal, M. Bragen, and P. Sydelko, "Complex Adaptive Systems Modeling with Repast Symphony, " *Complex Adaptive Systems Modeling*, Springer, Heidelberg, FRG (2013). <http://www.casmodeling.com/content/1/1/3>
- Railsback, S. F., & Grimm, V. (2011). *Agent-based and individual-based modeling: a practical introduction.* Princeton University Press.

- Ruderman D, 1997, "Origins of scaling in natural images" *Vision Research* 37 3385–3398
- Ruderman D, Bialek W, 1994, "Statistics of natural images: scaling in the woods" *Physical Review Letters* 73 814–818
- Sander, L. M. (2000). Diffusion-limited aggregation: a kinetic critical phenomenon?. *Contemporary Physics*, 41(4), 203-218.
- Sato T, Matsuoka M, Takayasu H, 1996, "Fractal image analysis of natural scenes and medical images" *Fractals* 4 463–468
- Shukla V and Waddell P (1991) Firm location and land use in discrete urban space: A study of the spatial structure of Dallas-Fort Worth, *Regional Science and Urban Economics*, 21, pp. 225-253
- Spehar, B., & Taylor, R. P. (2013). Fractals in art and nature: why do we like them?. In *IS&T/SPIE Electronic Imaging* (pp. 865118-865118). International Society for Optics and Photonics.
- Stewart, J. Q., & Warntz, W. (1958). Physics of population distribution. *Journal of regional science*, 1(1), 99-121.
- Thomas, I., Frankhauser, P., & De Keersmaecker, M. L. (2007). Fractal dimension versus density of built-up surfaces in the periphery of Brussels*. *Papers in regional science*, 86(2), 287-308.
- Thomas, I., Frankhauser, P., & Biernacki, C. (2008). The morphology of built-up landscapes in Wallonia (Belgium): A classification using fractal indices. *Landscape and Urban Planning*, 84(2), 99-115.
- Thomas, I., Frankhauser, P., Frenay, B., & Verleysen, M. (2010). Clustering patterns of urban built-up areas with curves of fractal scaling behaviour. *Environment and planning. B, Planning & design*, 37(5), 942.
- Van de Sande, A. (2004) Review: How long is the coastline of Britain. Courtesy of Alexandre Van de Sande at wanderingabout.com
- van Vliet, J., Hurkens, J., White, R., & van Delden, H. (2012). An activity-based cellular automaton model to simulate land-use dynamics. *Environment and Planning-Part B*, 39(2), 198.

- Vudec R, 1997, "Image segmentation using fractal dimension", GEOL 634, Cornell University, <http://www.cs.berkeley.edu/Richie/g634fin.ps.gz>
- White, R., & Engelen, G. (1993). Cellular automata and fractal urban form: a cellular modelling approach to the evolution of urban land-use patterns. *Environment and planning A*, 25(8), 1175-1199.
- Wang, H., Su, X., Wang, C., & Dong, R. (2011). Fractal analysis of urban form as a tool for improving environmental quality. *International Journal of Sustainable Development & World Ecology*, 18(6), 548-552.
- Wilensky, U. (1999). NetLogo. <http://ccl.northwestern.edu/netlogo/>. Center for Connected Learning and Computer-Based Modeling, Northwestern University, Evanston, IL.
- Wolfram, S. (1984). Universality and complexity in cellular automata. *Physica D: Nonlinear Phenomena*, 10(1), 1-35.
- Wu, F. (1999). Intrametropolitan FDI firm location in Guangzhou, China A Poisson and negative binomial analysis. *The Annals of Regional Science*, 33(4), 535-555.
- Yang Z, Purves D, 2003, "A statistical explanation of visual space" *Nature Neuroscience* 6 632–640
- Yarish M (1998) Intrametropolitan location of new office firms in Metropolitan Toronto. Unpublished Masters Thesis, School of Geography and Geology, McMaster University, Hamilton, Ontario.

Appendix 1: Fractal Metrics

| Fractal Dimension Index | Definition | Credit | Applicable to | Drawbacks | Calculation | Illustration |
|--|--|-------------------------|---|--|---|--|
| Fractal Dimension (D), (FRACT) | fractal dimension indicates the extent to which the fractal object fills the Euclidean dimension | Mandelbrot (1977, 1982) | Single patches natural planar shapes | -Only for single patches -dependent upon patch/cell size and/or the units | $\log P = 1/2D * \log A$ (P =perimeter, A = area) | <p>Fractal Dimension = 1 Fractal Dimension = 2</p> <p>Fractal Dimension = 3 Fractal Dimension = 1.58</p> |
| Mean Shape Index (MSI) | perimeter-to-area ratio (PARA). | Godron (1986) | | varies with the size of the patch (improved by Shape index, Patton-1975) | $ED=E/A$ (E=total edge; A=total area) | <p>ED: 800m/ha ED: 1260m/ha</p> <p>Class areas are identical</p> |
| Mean patch fractal (MPFD) | | FRAGSTATS | | | | |
| Double log fractal dimension (DLFD) | | FRAGSTATS | | | | |
| perimeter-area fractal dimension (PAFRAC) | describes how patch perimeter increases per unit increase in patch area | FRAGSTATS | | Not for small size samples (relies on regression method) | $A = k P^2/D$, where k is a constant (Burrough 1986) | |

| | | | | | | |
|--|---|-----------------------------|--|--|--|---|
| Area Weighted Mean Patch Fractal Dimension (AWMPFD) | weighting patches according to their size | (Krummel, 1987) | Class and landscape level | | | |
| medial axis transformation (MAT) | derived from a depth map of the patch, where each pixel value represents the distance (in pixels) to the nearest edge | (Gustafson and Parker 1992) | Coupled with linearity index (LINEAR) | | | |
| Related circumscribing circle (CIRCLE) | uses smallest circumscribing circle instead of the smallest circumscribing square | FRAGSTAT | Simpler to implement Applicable for vector data | | | |
| Deterministic Leapfrogging Fractality | fractal that is a result of growth process by leapfrogging at several scales | (Benguigui, 2004) | Applicable for vector data | | $D = \frac{\ln[(b/c)^2 + n]}{\ln(1/c)}$ <p>D is the fractal dimension of the deterministic fractal and it has the typical fractal relation</p> $N(lk) = lk^{-D}$ |  |

Appendix 2: Size-Distribution of Urban Form in Kitchener-Waterloo

